CHAPTER 3

Effect of 140 MeV Ag^{+11} ion irradiation on conductive additives filled in PMMA polymer matrix

This chapter describes the characterization of three polymer composites prepared by dispersion of conductive fillers i.e carbon black (CB), Aluminum (Al), copper (Cu) in PMMA matrix. These composites were irradiated with 140 MeV Ag+11 ions at different fluences. The various results of experimentations before and after ion beam irradiation are presented. Scientific explanations of various properties e.g. electrical, structural, thermal properties and surface morphology of conductive composites are discussed.

3.0 Introduction

In recent years, there is an increasing interest in the flexible polymer composites with high dielectric constant because they possess important technological applications in certain areas. Such composites are attractive as potential materials for high charge-storage capacitor, electrostriction artificial muscles, "smart skins" for drag reduction, and microfluidic systems for drug delivery [1–8]. The effective dielectric constant of polymer composites can be improved dramatically by incorporating electrical conducting phase into the polymer matrix as the concentration approaches the percolation threshold [9–13]. However, many properties of the composite still remain unknown even despite numerous studies have been carried out in the past few years [6]. A well-known fact about conductor–insulator system is the drastic change in the electrical conductivity of these composites in a narrow range of concentration of the conducting phase. This sudden change in the relationship between electrical conductivity and filler concentration is attributed to the formation of continuous chains or network of the conducting phase that spans throughout the insulating matrix. This phenomenon involving the change in the dispersion state of the conducting phase is usually explained by percolation theory and is known as percolation. The minimum volume content of the conducting filler at which the drastic change in electrical conductivity begins is referred to as the percolation threshold. According to the percolation model, the electrical properties such as electrical conductivity and dielectric constant of conductor–insulator systems should exhibit a power law dependency on the magnitude of the difference $(P - P_c)$, where P denotes the volume fraction of the conducting phase and P_c stands for the percolation threshold. It has also been shown that the dielectric constant of metal–insulator systems might exhibit divergent behavior near the percolation threshold [7,14-16].

Ion irradiation of polymers and polymer composites can induce irreversible changes in their macroscopic properties. Electronic excitation, ionization, chains scission and cross-links as well as mass losses are accepted as the fundamental events that give rise to the observed macroscopic changes [17]. In solids high energy heavy ion loses energy mainly through electronic processes and the energy deposition centered in a very small range that is referred to as tracks. This chapter describes the dependence of various properties of polymer composites on filler concentration and fluence ($1x10^{11}$ ions/cm^2 and $1x10^{12}$ ions/cm^2) of silver ion beam. The effects of 140MeV silver ion irradiation on following composites have been investigated in this chapter.

(1) Carbon black/PMMA composites [18]

(2) Al/PMMA composites [19]

(3) Cu/PMMA composites [20, 21]

The radiation induced changes in dielectric, structural, thermal properties and surface morphology of composites were studied using impedance /gain phase analyzer, X- ray diffraction (XRD), Differential scanning calorimetry (DSC), scanning electron microscopy (SEM) and atomic force microscopy (AFM).

3.1 Carbon black filled PMMA composites: Results and discussion

3.1.1 Electrical properties

Dielectric analysis measures two fundamental electrical characteristics of materials: the capacitive (insulating) nature, which represents its ability to store electrical charge; and the conductive nature, which represents its ability to transfer electric charge. Through the dielectric analysis, the dielectric constant and dielectric loss (tangent) and ac conductivity of a material can be obtained. The electric properties of a material as a function of frequency, filler concentration, ion fluence and also temperature dependence electrical properties of pure sample in the temperature range

25-80^{0}C are discused. The ac conductivity and dielectric constant were calculated using equations (2.4.25) and (2.4.12) respectively as discussed in chapter-2.

(a) Frequency dependence ac conductivity

The a.c. conductivity of the composites as a function of the frequency, fluence, and filler concentration has been studied and shown in figure 3.1(a-c). The conductivity of composite increased with concentration of filler that is possibly due to the electronic interaction process taking place in the composites and therefore resulted composites show more conductive with the increase of the filler content [21]. At low filler content, the conducting particles are separated and electrical charge may flow only by means of hopping or tunneling through a non conducting medium between the neighboring particles. The transport of charge carriers would be inefficient and the overall conductivity of composite was observed to be low at lower concentration (Fig 1). When particle concentration increases, the gap between the particles diminishes and conductivity slowly increases due to increase of conduction path [22,23]. At the percolation threshold conductivity increased steeply as shown in Fig. 3.1d. The conductivity of composites was found to increase after irradiation (Fig 3.1(b-d)). This result revealed that the irradiation of composite leads to the scissioning of polymer chains and resulted in hydrogen depleted carbon network due to emission of hydrogen and/or other volatile gases that contributed to increase the conductive nature of the composite [24].

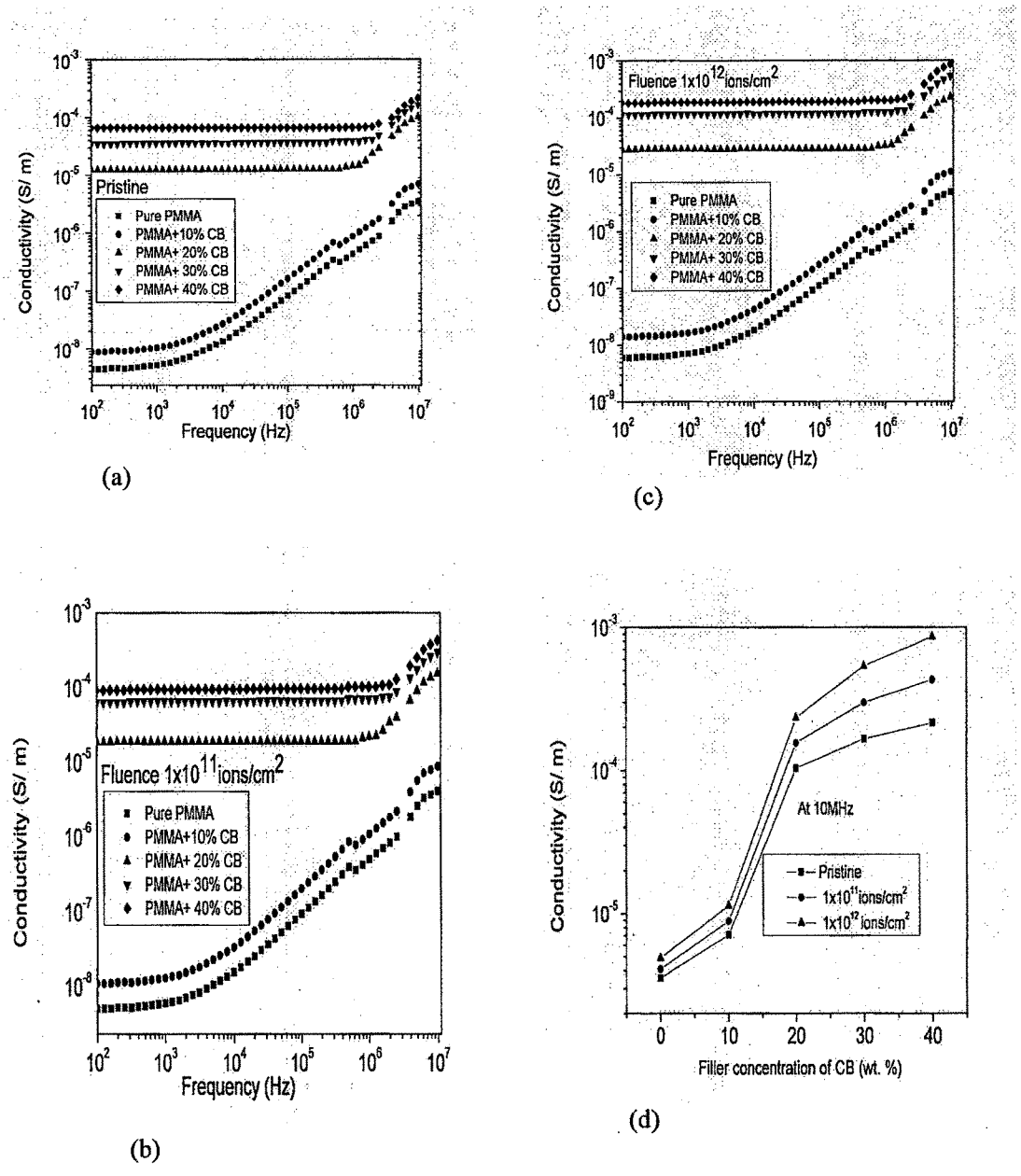

Fig.3.1 Conductivity vs. frequency for PMMA/ CB composites (a) Pristine and (b) Irradiated at a fluence $1x10^{11}$ions/cm^2 (c) Irradiated at a fluence $1x10^{12}$ions/cm^2 (d) Conductivity vs. filler concentration at 10MHz.

(b) **Temperature dependence ac conductivity**

Figure 3.2 shows the variation of conductivity of polymer composites with frequency of applied electric field, concentration and temperature for all pristine samples. The rise of conductivity upon increasing the frequency and temperature is a common respond for polymeric and semiconductor materials [25]. Conductivity increases with filler concentration and also with temperature. Figure 3.3 shows the variation of ln (Ac-conductivity) with the inverse temperature for all samples at fixed frequency (10 KHz and 1 MHz). The conductivity increased with increasing temperature and this behavior can be explained by suggesting that the electronic charge must hop between conducting particles. In other word, the increment in temperature provides an increase in free volume and segmental mobility [26].

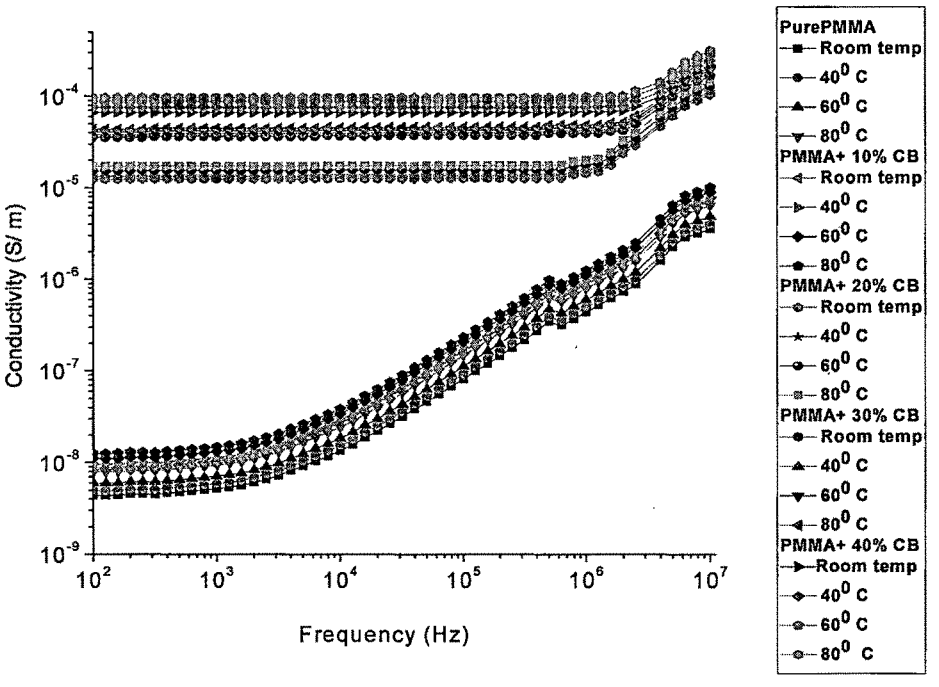

Fig. 3.2 Variation of conductivity of PMMA/CB composites with frequency of applied electric field, concentration and temperature.

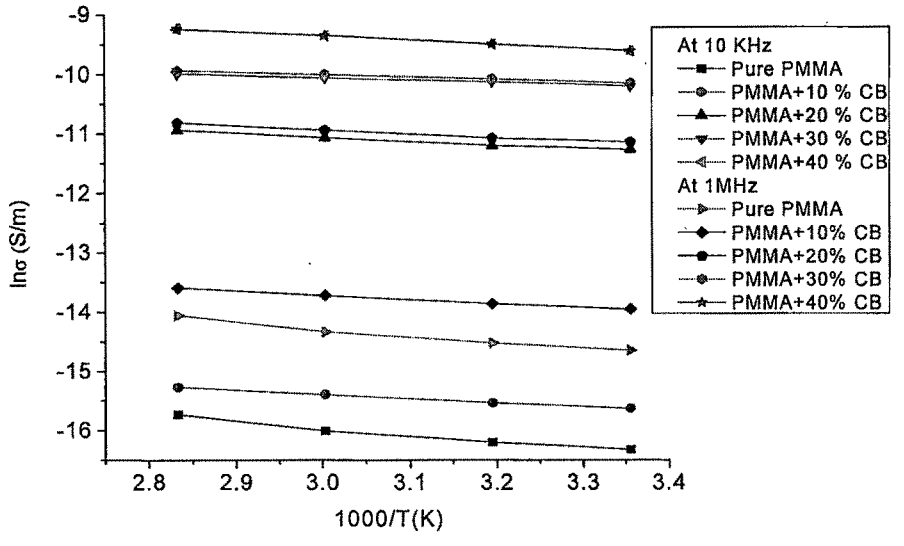

Fig. 3.3 Plot of natural log of conductivity (lnσ) versus inverse temperature, 1000/T [K] for PMMA/CB composites.

(c) Frequency depedance dielectric constant

The dielectric constant of PMMA/CB composites with frequency is shown in Fig. 3.4(a-d). The general trend of the curves shows the increase in dielectric constant with the filler concentration. The increase in the dielectric constant with filler content related with interfacial polarization effect between polymer and filler particles. The polarization also contributed to the charge quantity. From this point of view, the dielectric constant of the composites was higher than that of the pure polymer [27]. At low frequency, below 500 Hz, dielectric constant shows a sharp increase, it could be possibly associated with Maxwell-Wagner mechanism (interfacial space charge) and electrodes polarization effect [28]. At low frequencies, accumulations of electronic impurities and space charges also have similar effects. These effects possibly caused large and rapid increase in dielectric constant [28, 21]. It is also observed that dielectric constant remains constant up to 10MHz. This reveals that the motion of

charge carriers is constant in this frequency range. The dielectric constant value was also found to increase after irradiation (Fig.3.4(b-c)). The increase in dielectric constant upon irradiation suggests that the sccissioning of polymer chain created free radicals and unsaturation etc. in the composites. It resulted an increase in interfacial polarization of space charges and therefore dielectric constant of composites was found to increase after irradiation.

(d) Temperature dependence dielectric constant

Figure 3.5 shows the variation of dielectric permittivity of polymer composites with frequency of applied electric field at different concentrations and temperatures for pristine samples. The dielectric constant attains high value at low frequency and decreases with increasing in frequency. The decrease of dielectric constant is mainly attributed to the mis-match of interfacial polarization of composites to external electric field at elevated frequencies [29]. Dielectric constant remains constant beyond a frequency of 10^3 Hz for all composites, but its magnitude increases as filler concentration increases. The dielectric constant as a function of temperature is shown in Fig. 3.6 at two different frequencies. It can be seen that the dielectric constant increases with increasing temperature. The enhancement of the dielectric constant with increasing temperature can be attributed to segmental mobility of the polymer, facilitate the orientation of dipoles and consequently increase dielectric constant [30].

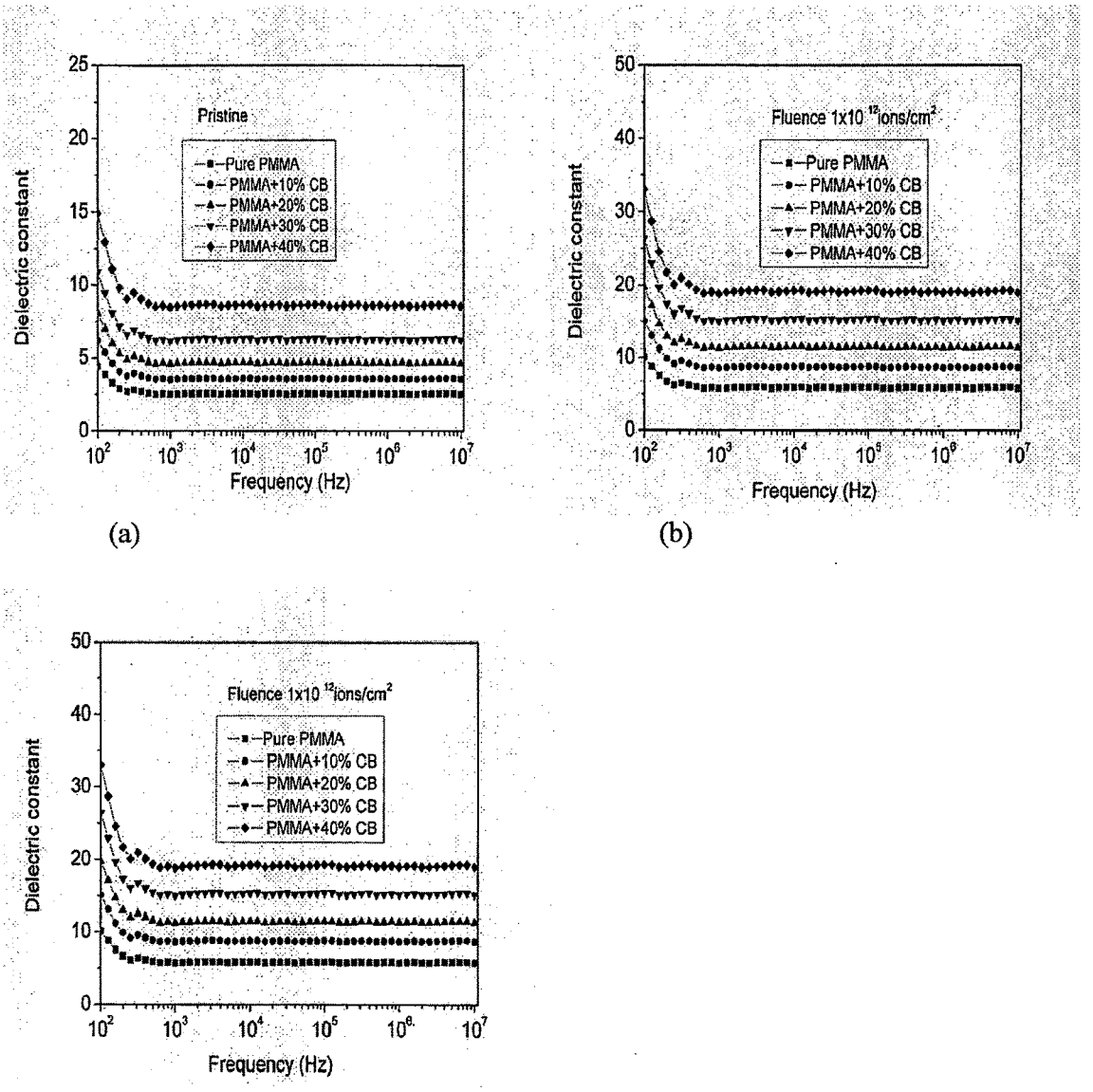

Fig.3.4 Dielectric constant vs. frequency for PMMA/CB composites (a) Pristine and (b) Irradiated at a fluence $1x10^{11}$ions/cm^2 (c) Irradiated at a fluence $1x10^{12}$ions/cm^2.

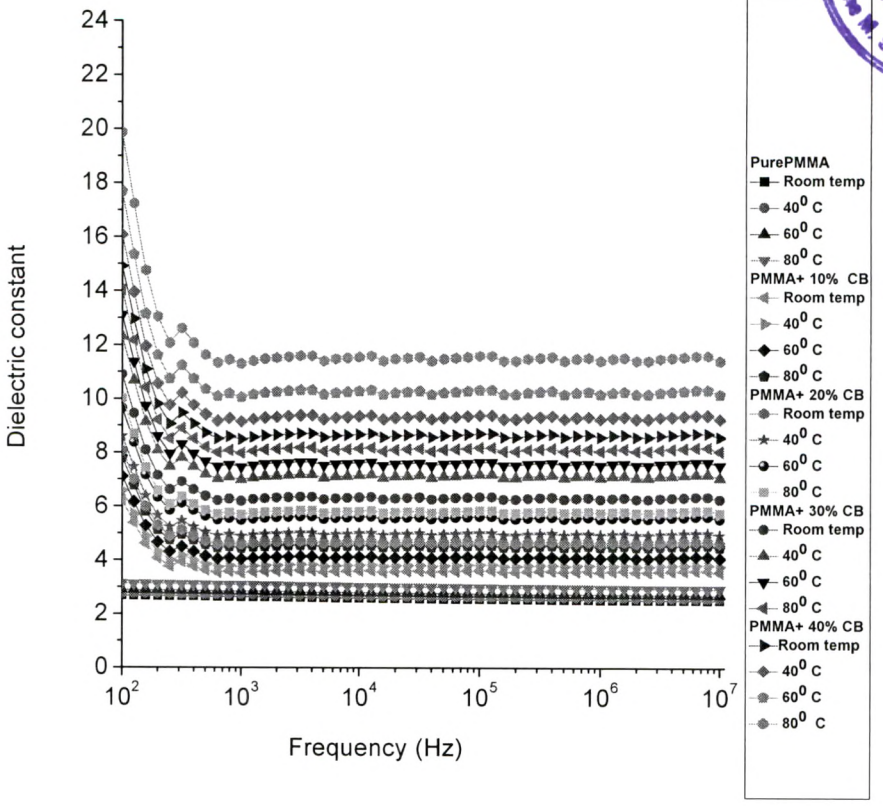

Fig. 3.5 Variation of dielectric constant of PMMA/CB composites with frequency of applied electric field, concentration and temperature.

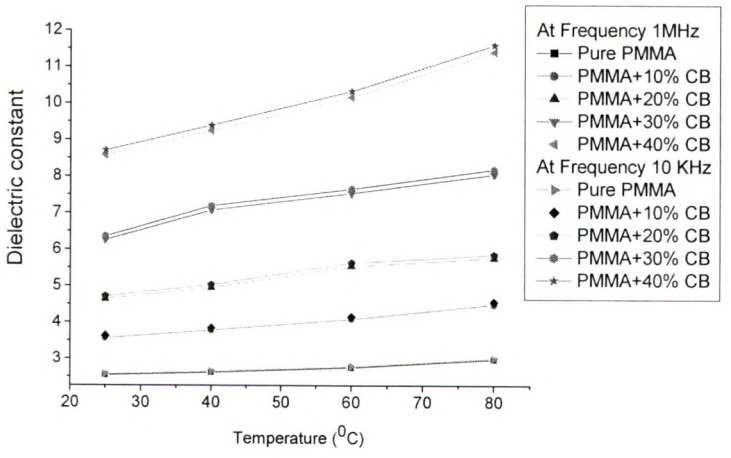

Fig.3.6 Variation of dielectric constant vs temperature at different concentrations of PMMA/CB composites at two different frequencies.

(e) Frequency dependence dielectric loss

The dielectric loss is the power dissipated in dielectric as a heat when the dielectric is exposed to an electric field. Dielectric loss (tanδ) is defined as a ratio of energy lost or dissipated per cycle to the energy stored. It was measured directly using Impedance gain phase analyzer. Fig 3.7(a-c) represents the dielectric loss versus frequency for pristine and irradiated samples. It is observed that the dielectric loss decreases exponentially with increasing the frequency and then became less dependent at higher frequency. It is also observed that the loss factor increases moderately with carbon black concentration and also with the ion fluence. The growth in tan δ and thus increase in conductivity is brought about by an increase in the conduction of residual current and absorption current [31].

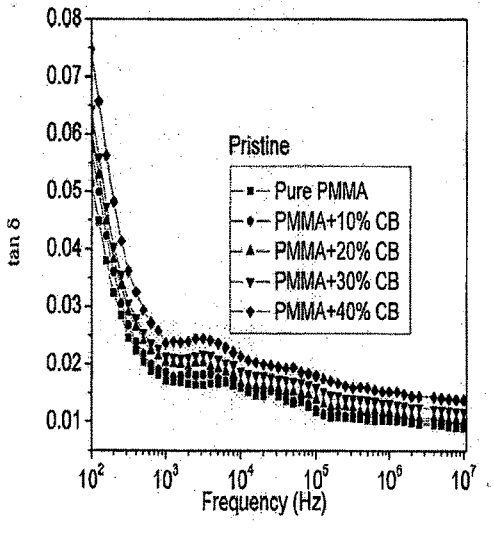

(a)

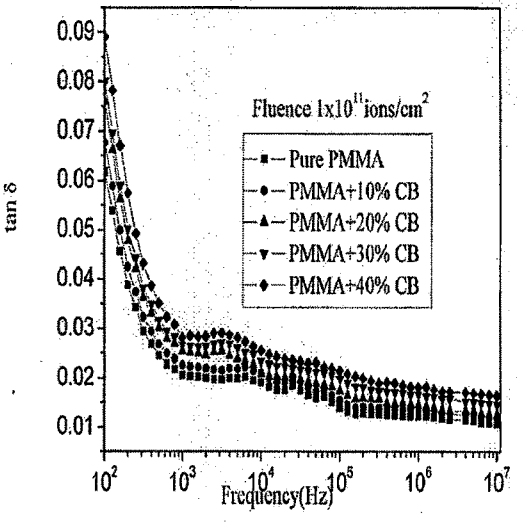

(b)

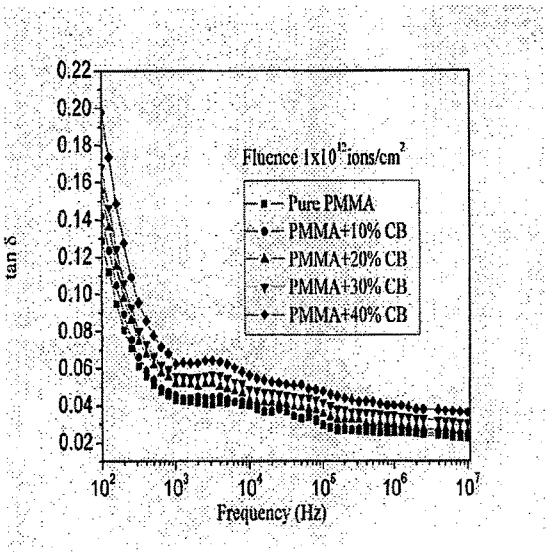

(c)

Fig.3.7 Dielectric loss vs. frequency for PMMA/CB composites (a) Pristine and (b) Irradiated at a fluence $1x10^{11}$ions/cm^2 (c) Irradiated at a fluence $1x10^{12}$ions/cm^2 .

(f) Temperature dependence dielectric loss

Figure 3.8 shows the variation of dielectric loss of PMMA/CB composites with frequency of applied electric field, concentration and temperature for all pristine samples. Fig. 3.9 depicts the dielectric loss as a function of temperature at two different frequencies for pure PMMA and CB filled polymer composites with different concentrations of CB. From Fig.3.9, it can be seen that the dielectric loss factor increases with increase in temperature. The dielectric loss is due to the perturbation of phonon system by an electric field, the energy transferred to the phonon is dissipated in the form of heat.

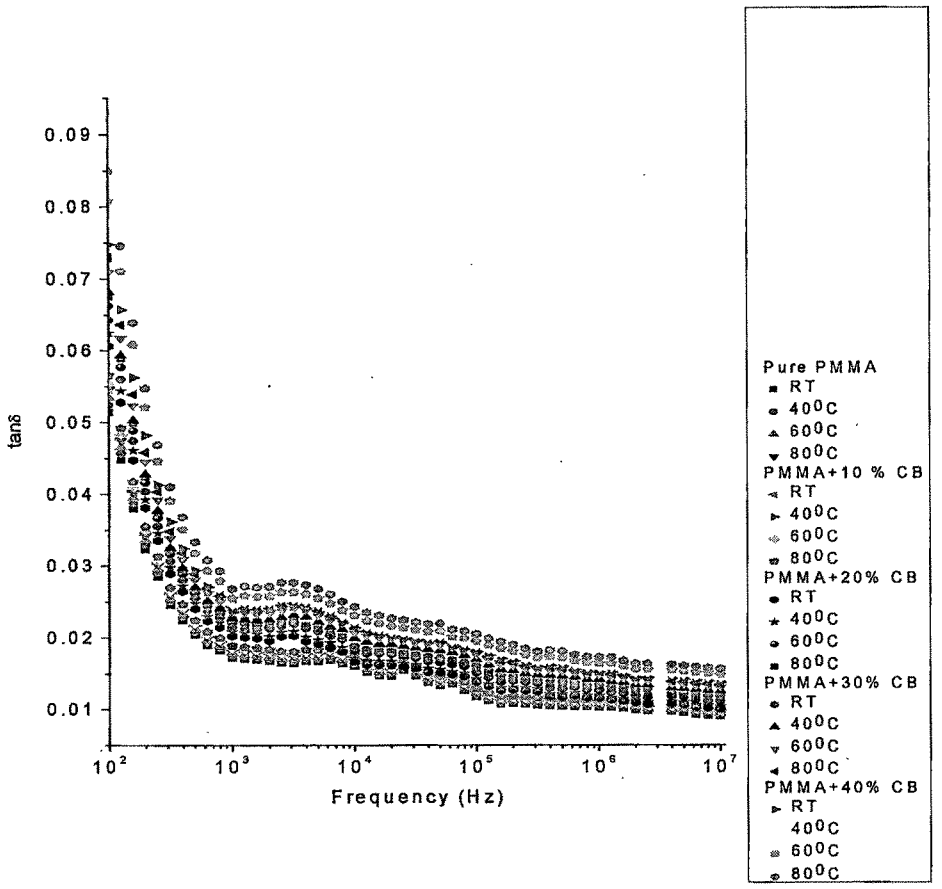

Figure 3.8 Variation of dielectric loss of PMMA/CB composites with frequency of applied electric field, concentration and temperature.

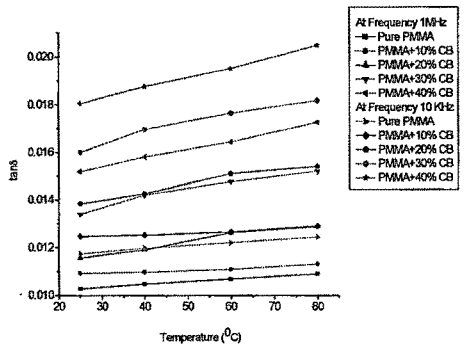

Fig. 3.9 Variation of dielectric loss vs temperature with different concentrations of PMMA/CB composites at two different frequencies.

3.1.2 X-ray diffraction analysis

The XRD patterns for pristine and irradiated composite films were recorded at different concentrations of filler (Fig. 3.10). The diffraction patterns showed the amorphous nature of the composites. The prominent X-ray peak was observed at 2θ =25.97^0 and consistent with different concentration of CB in polymer (Fig, 3.10 (a-c)). This peak perhaps due to the presence of CB particles in the polymer matrix. The irradiated ones also show an identical diffraction pattern except that the decrease in the intensity of the peak due to irradiation. Although the intensity of the diffraction peak decreases due to irradiation, but no significant change in peak position is observed. It reveals that the sample became more amorphous in nature after irradiation and also indicates that there is no change in lattice parameter.

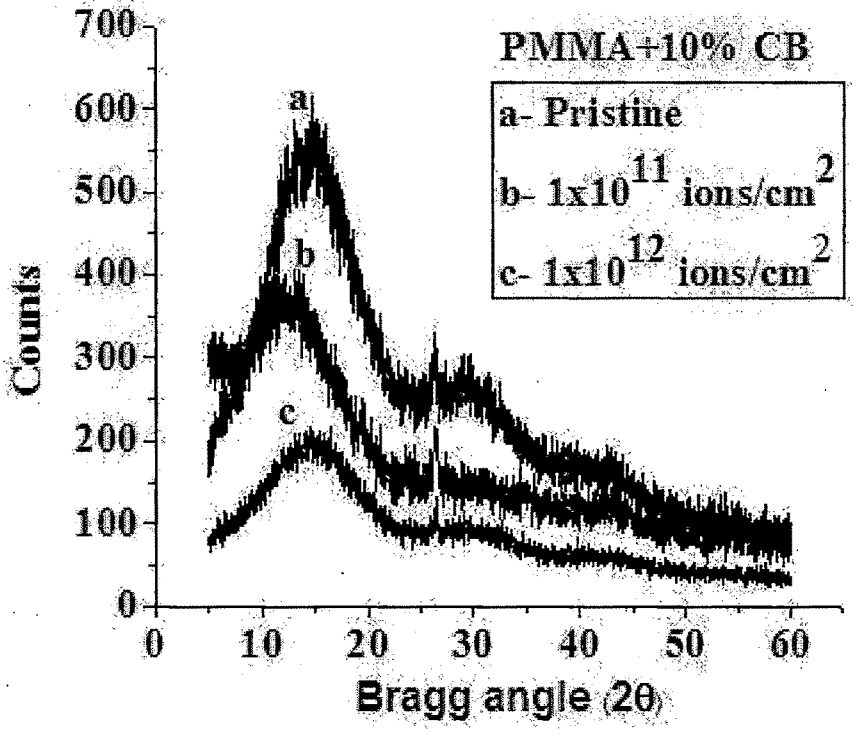

Fig. 3.10 (a) XRD spectra of pristine and irradiated samples for PMMA+10% CB composite.

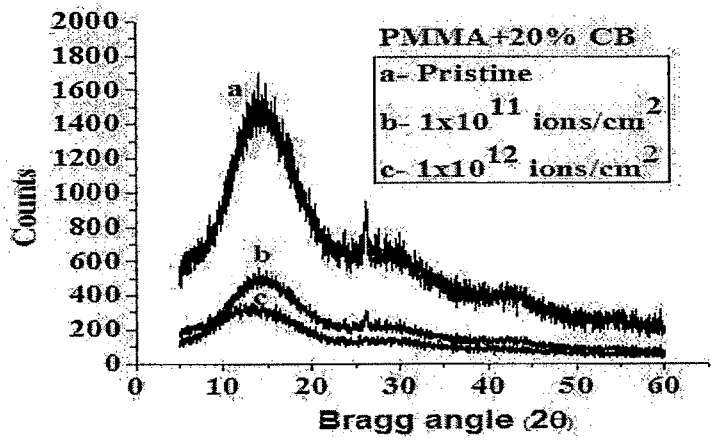

Fig. 3.10 (b) XRD spectra of pristine and irradiated samples for PMMA+20% CB composite.

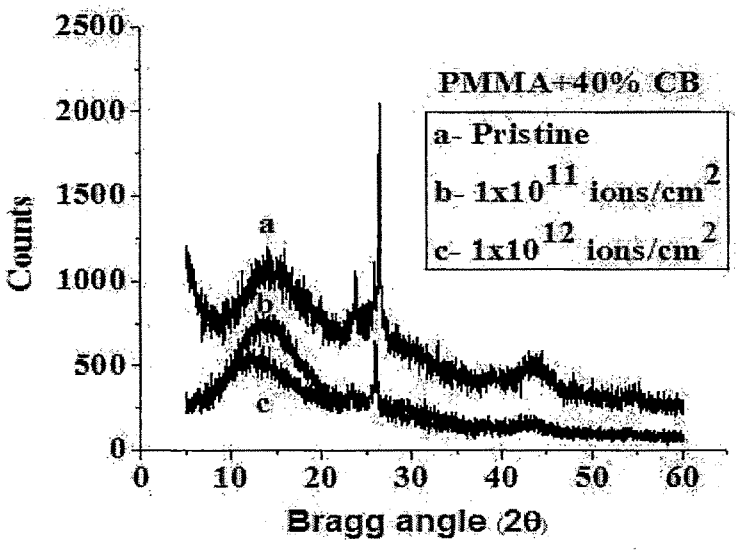

Fig. 3.10 (c) XRD spectra of pristine and irradiated samples for PMMA+40% CB composite.

3.1.3 Differential Scanning calorimetry(DSC) analysis

DSC instruments are widely used for the thermal characterization of polymers/polymer composites. A differential scanning calorimetry (DSC) experiment was performed using a reference material and a predetermined heating (or cooling) rate was imposed to the system with a given temperature excursion (40^0 to 150^0 ^{0}C). The sample followed the temperature of the reference and the heating power difference between the sample and reference was recorded. To study the irradiation effects on thermal property of the composite, the DSC thermogram of pure PMMA as a reference was recorded (Fig. 3.11). DSC thermograms of PMMA+40% CB composite before and after irradiation were also recorded (Fig. 3.11). It was found that when the concentration of CB was increased in the polymer matrix, glass transition temperature (T_g) shifted to higher temperature, resulting in the cross linking of polymer and CB particles. After irradiation, it was found that T_g shifted to lower temperature. It reveals that the ion irradiation leads to polymer chain scissioning and subsequently reduction in molecular weight. As a result, system moved towards the more disordered state, which is also corroborated with XRD results.

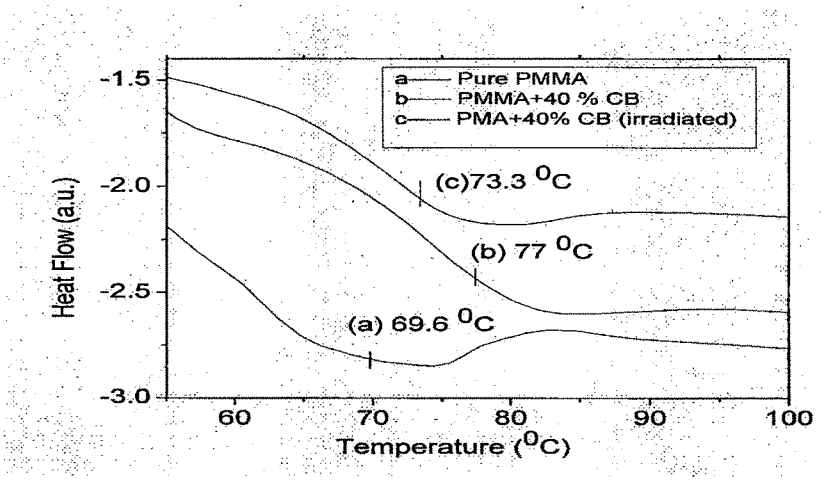

Fig.3.11. DSC thermograms of (a) pure PMMA pristine (b) PMMA+40% CB pristine (c) PMMA+40%CB (irradiated).

3.1.4 Surface morphology

(i) Atomic force microscopy(AFM)

The AFM image of 10 × 10 μm^2 area was recorded in tapping mode as shown in Fig. 3.12 (a-d). Each AFM image was analyzed in terms of surface average roughness (R_a). It is observed that roughness increases from 4.2nm to 23.8 nm with carbon black concentration of 10% and 40% and also further increases from 7.2 nm to 42.2 nm respectively after irradiation at a fluence of $1x10^{12}$ ions/cm^2. The increase in surface roughness (R_a) with increasing filler concentration was observed due to the increase in density and size of conducting particles on the surfaces of the polymeric films [32]

(i) Scanning electron microscopy (SEM)

SEM images were examined to observe the change in the texture of the fractured surface of the composites. It is seen that the CB particles are isolated at 10% of concentration which indicates that there is no interaction between them (Fig. 3.13 a). As the CB content was increased (i.e. 40% CB-filler), clusters of CB particles were found (Fig. 3.13c).These clusters might be considered a region in the polymer matrix, where particles are in physical contact or very close to each other. Aggregations of these micro clusters were observed on the surface after irradiation (Fig. 3.13 b, d).

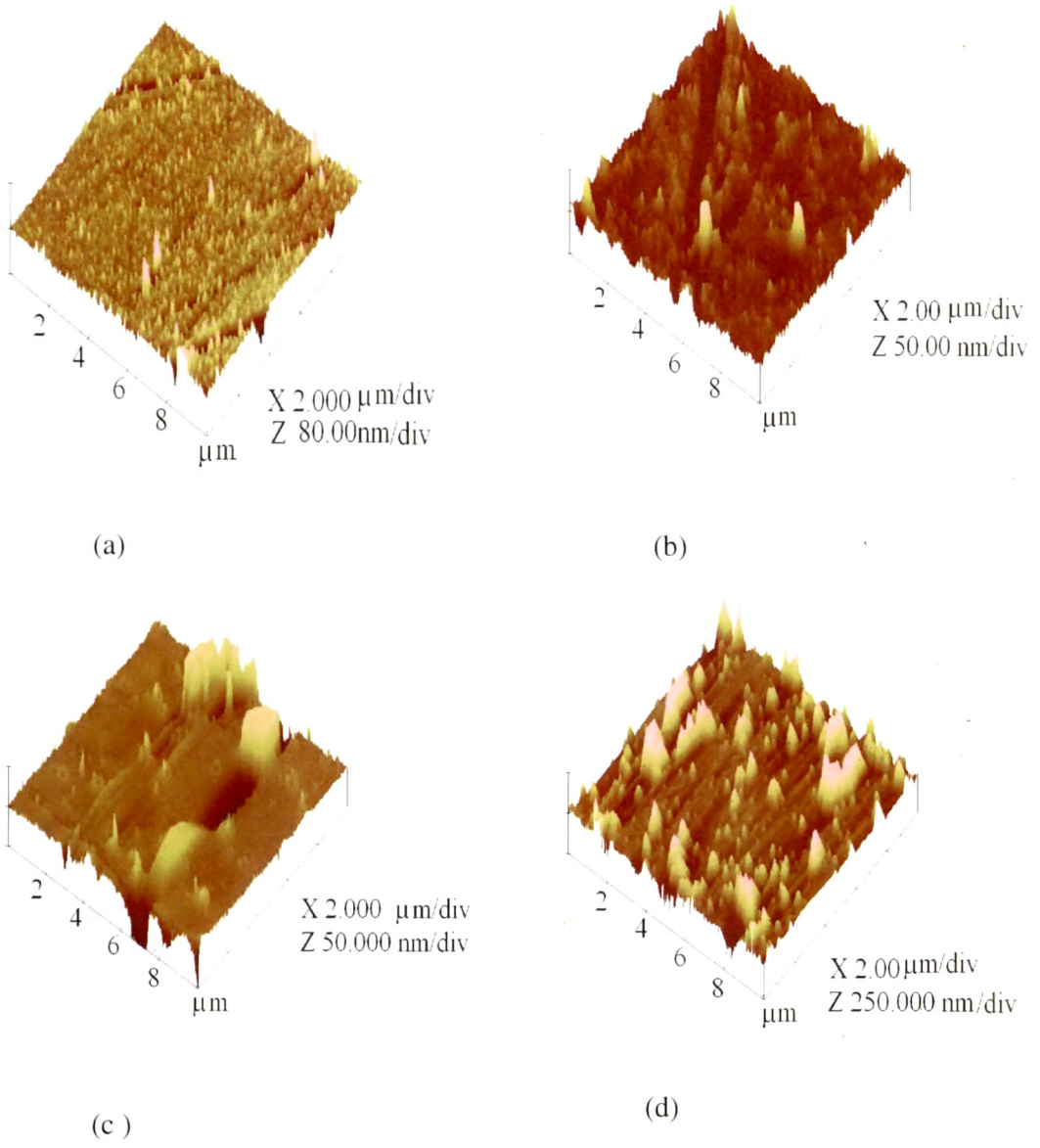

Fig. 3.12. AFM images of PMMA+10% CB (a) pristine (b) at 1 × 10^{12} ions/cm^2 and PMMA+40% CB (c) pristine (d) at 1 × 10^{12} ions/cm^2.

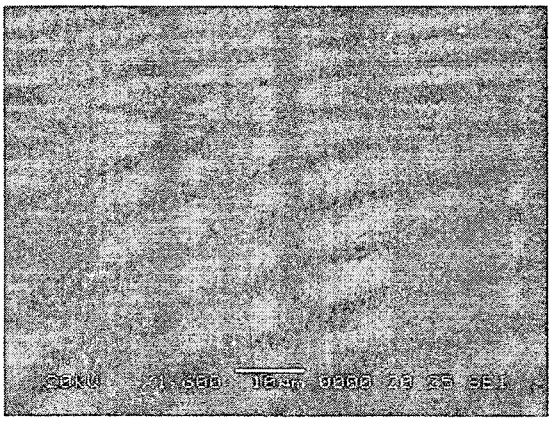

(a)

(b)

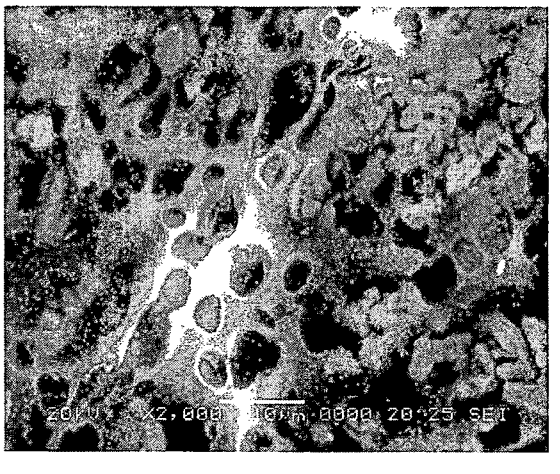

(c)

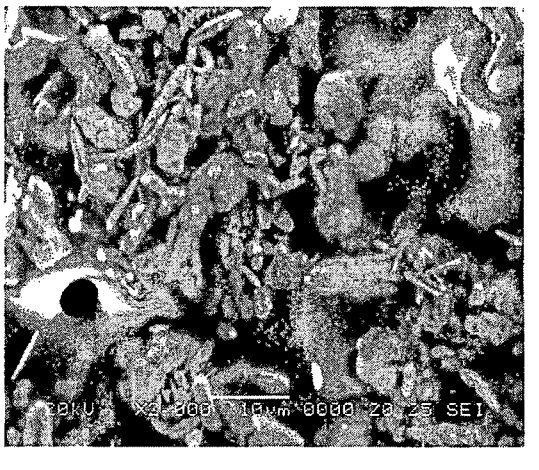

(d)

Fig. 3.13 SEM images of PMMA+10% CB composite (a) pristine (b)irradiated at 1×10^{12} ions/cm^2 and PMMA+40% CB composite (c) pristine (d) irradiated at 1×10^{12} ions/cm^2.

3.1.5 Conclusions

Swift heavy ion irradiation has significantly changed the electrical, structural, thermal properties and surface morphology of the carbon black filled PMMA composites. This is attributed to the fact that the radiation exposure on the polymer composite converts the polymeric structure in to hydrogen depleted carbon network and promotes good adhesion between carbon black particles and polymer. This makes the composite

more conductive and harder. The dielectric constant/loss shows frequency dependent behavior and change significantly after irradiation. The ac conductivity increased with increasing temperature and this behavior can be explained by suggesting that the electronic charge must hop between carbon black particles. The dielectric constant of the CB/PMMA composites increased with an increase in the temperature, which has been attributed to the segmental mobility of the polymer molecules. The X-ray diffraction patterns of the composites show an increase in amorphousity of polymer composite upon irradiation. DSC analysis revealed that the glass transitions temperature (T_g) shifted towards lower temperature upon ion irradiation and reveals that the composite system became disordered and amorphous in nature. The contact of the particles increased on increasing the concentration of filler and connectivity further increased upon irradiation as revealed from SEM analysis, its also confirmed by conductivity results.

3.2 Aluminum filled PMMA composites: Results and discussion

3.2.1 Electrical properties

(a) Frequency dependence ac conductivity

The dependence of effective ac electrical conductivity of PMMA/Al composites on frequency, filler content and ion fluence is shown in Fig 3.14 (a-c). Fig.3.14 d shows dependence of conductivity on filler concentration at a frequency of 10MHz. The conductivity is enhanced by increasing the applied frequency. This is due to the decrease in contributions of polarization effect at high applied frequency range [33, 34]. The conductivity increases on increasing the concentration of Al content. This is attributed to the electronic interaction processes and formation of conductive network due to aluminum particles contact that took place in the composites [35]. It is also observed that the conductivity increases with increasing the ion fluence. Irradiation is

expected to promote the metal to polymer bonding and convert the polymeric structure into a hydrogen depleted carbon network due to emission of hydrogen and /or other volatile gases. It is this carbon network that is believed to make the polymers more conductive [23].

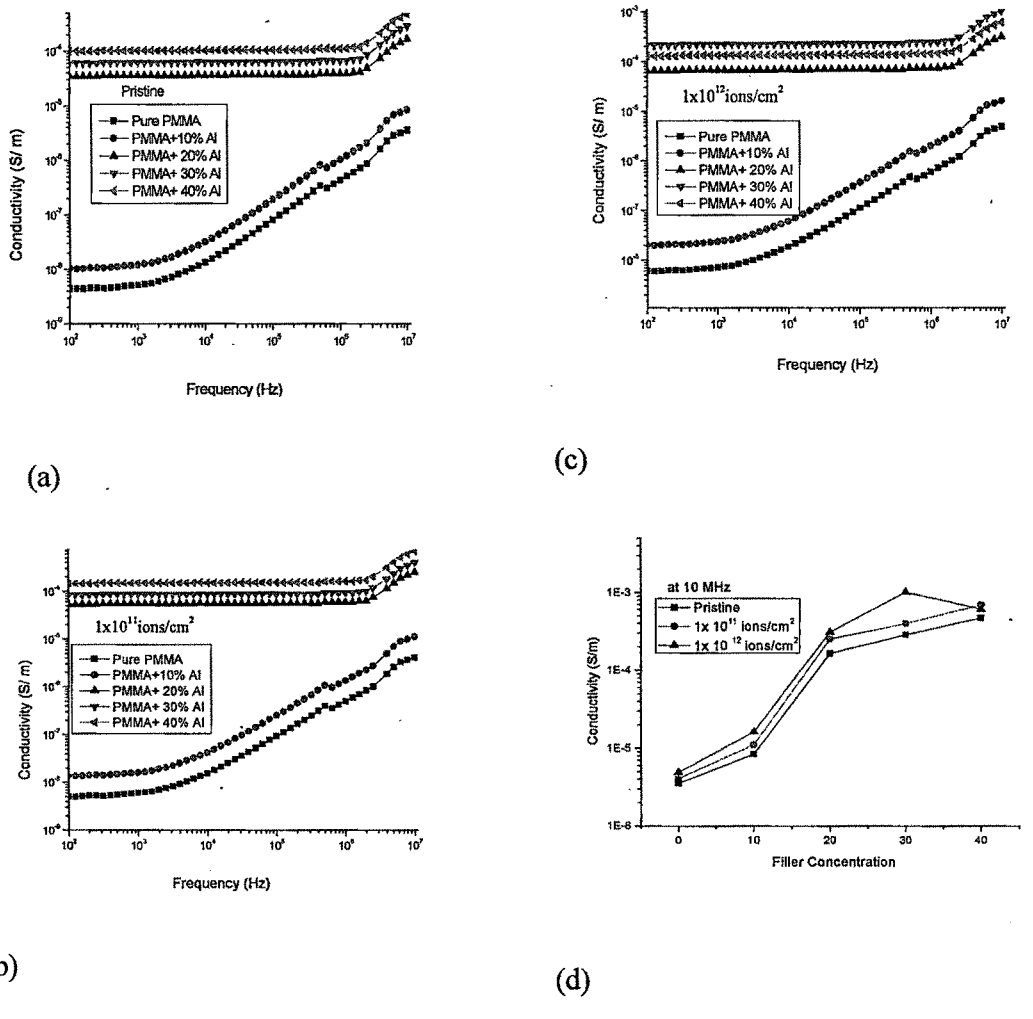

Fig.3.14 Conductivity vs. frequency for PMMA/Al composites (a) Pristine and (b) Irradiated at a fluence of $1x10^{11}$ions/cm^2 (c) Irradiated at a fluence of $1x10^{12}$ions/cm^2 (d) Conductivity vs. filler concentration at 10MHz.

(b) Temperature dependence ac conductivity

Figure 3.15 shows the variation of conductivity of polymer composites with frequency of applied electric field, concentration and temperature. The increase in conductivity with increasing the frequency and temperature is a common respond for polymer composites. It is due to the increase of the mobility of charge carriers in the composite. As shown in figure, there are two trends, the first one (from 100Hz to 1M Hz) is frequency independent conductivity and another (from 1MHz to 10M Hz) is frequency dependent conductivity for 20%, 30%, and 40% composites. The first trend is contributed by free charges available in the composite system whereas the second, which is frequency dependent conductivity, is due to trapped charges which are only active at higher frequency region [36, 37]. As shown in figure, 0 % and 10% samples behave as a insulating phase and after further doping at higher concentrations, samples show conducting behavior [38].

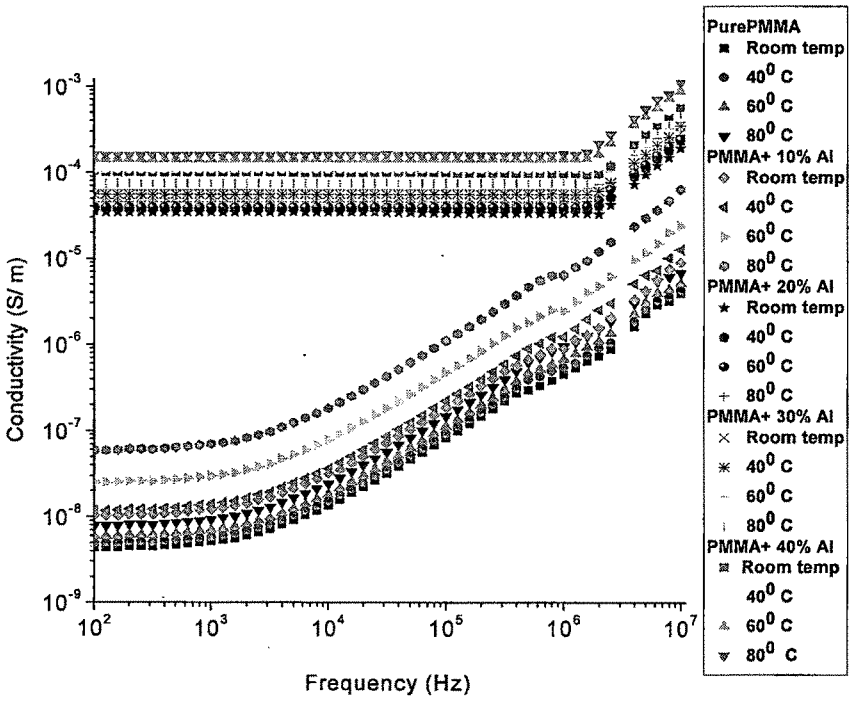

Fig.3.15 Variation of conductivity of PMMA/Al composites with frequency of applied electric field, concentrations and temperature.

Figure 3.16 shows the variation of ln (Ac-conductivity) with the inverse temperature for all pristine samples at fixed frequency (10 MHz). The conductivity increased with increasing temperature and this behavior can be explained by suggesting that the electronic charge must hop between metal particles. In other word, the increment in temperature provides an increase in free volume and segmental mobility.

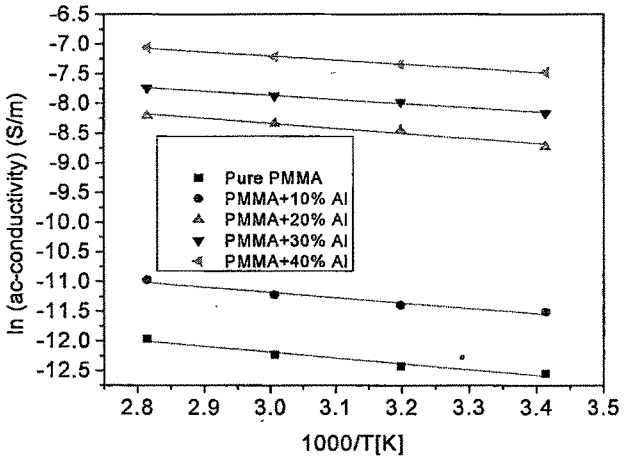

Fig.3.16 Plot of natural log of conductivity (lnσ) versus inverse temperature, 1000/T [K] for PMMA/Al composites.

(c) Frequency dependence dielectric constant

Figure 3.17 (a-c) shows an increase in dielectric permittivity of PMMA/Al composites with filler concentration and ion fluence. It is observed that the dielectric constant decreases moderately with frequency. As the frequency increases, the charge carriers migrate through the dielectric get trapped against a defect sites and induce an opposite charge in its vicinity, as a result of which they slow down and the value of dielectric constant decreases moderately [39].

The further increase in dielectric constant for irradiated samples may be attributed to the disordering of the material by means of chain scission in polymer composites and as a result, the increase in the number of free radicals, unsaturations etc. As the fluence increases the dielectric constant also increases.

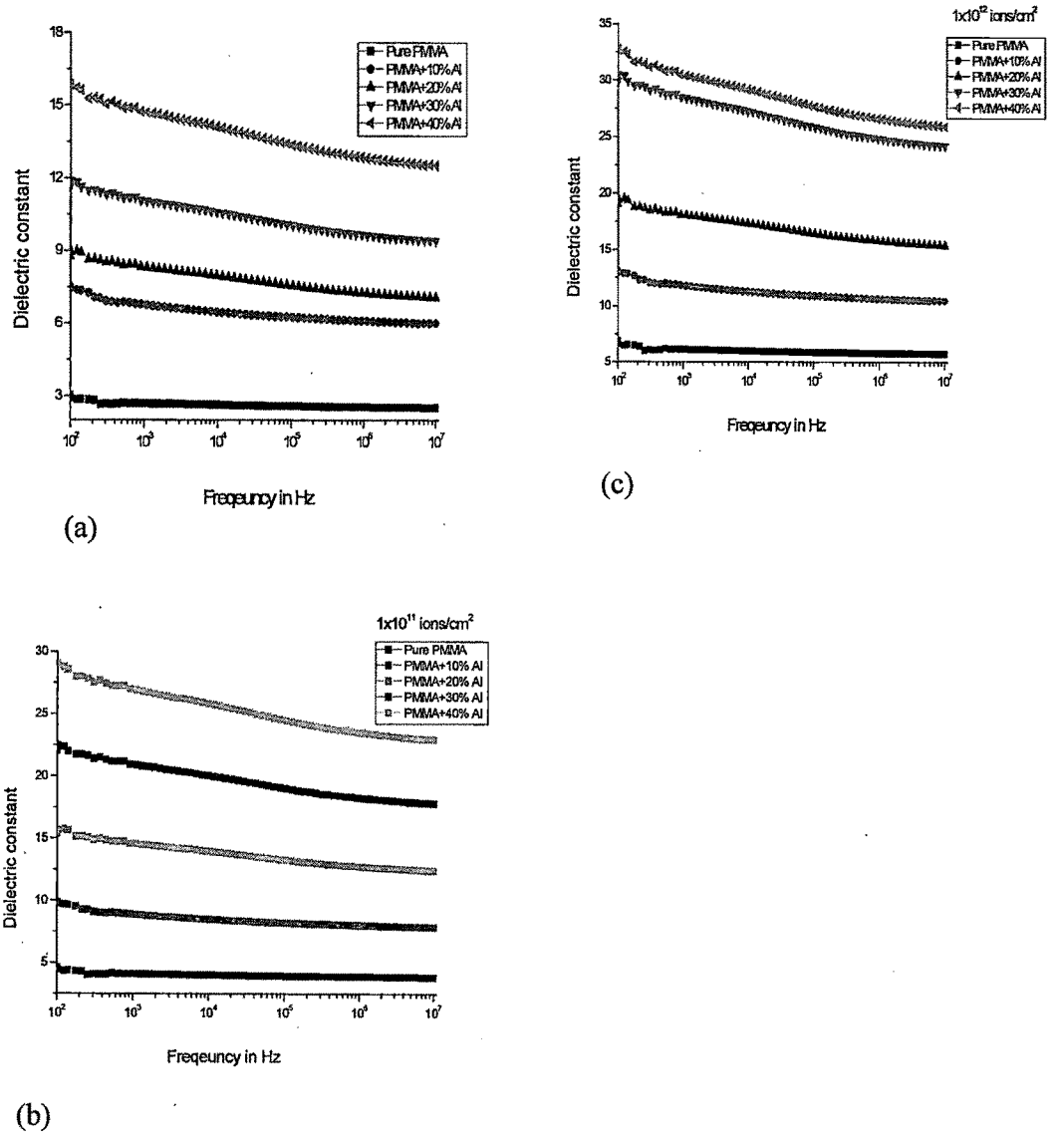

Fig.3.17 Dielectric constant vs. frequency for PMMA/Al composites (a) Pristine and (b) Irradiated at a fluence of $1x10^{11}$ions/cm^2 (c) Irradiated at a fluence of $1x10^{12}$ions/cm^2.

(d) Temperature dependence dielectric constant

Figure 3.18 shows the variation of dielectric permittivity of polymer composites with frequency of applied electric field, concentration of filler and temperature.

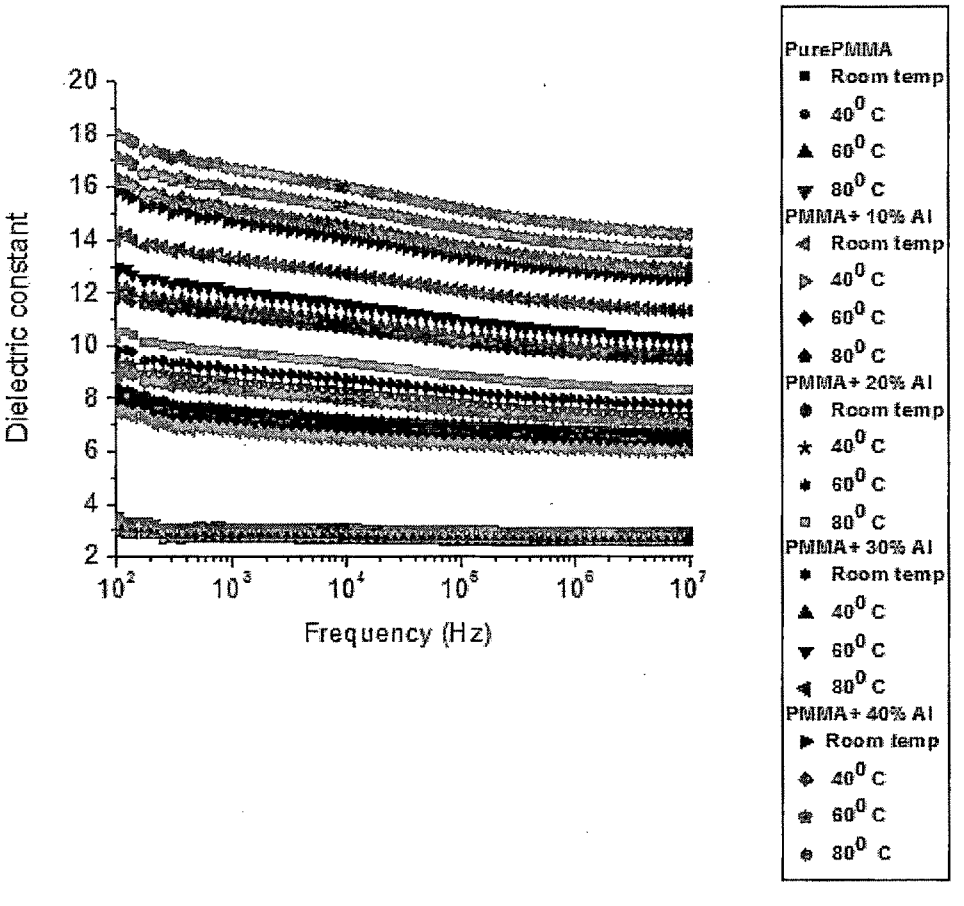

Fig 3.18 Variation of dielectric constant of PMMA/Al composites with frequency of applied electric field, concentration and temperature.

Figure 3.19 shows the variation of dielectric constant with temperature at 10 kHz and 1 MHz frequencies for different concentration of polymer composites. The PMMA/Al composites display a increasing tendency in dielectric constant on increasing the temperature. This phenomenon is explained from the occurrence of two kinds of behaviors, which would yield converse effects on dielectric constant of the composite by changing the temperature [40]. First, increasing temperature would improve the

segmental mobility of the polymer, facilitate the orientation of dipoles and increase dielectric constant consequently. Second, the obvious differential thermal expansion of the Al metal and polymer can disrupt the clusters of metal particles, which results in a decrease in the dielectric constant as the thermal expansion coefficient of the polymer is greater than that of the Al metal. But in the present case the increase of dielectric constant with temperature can be said that segmental mobility is the dominant process.

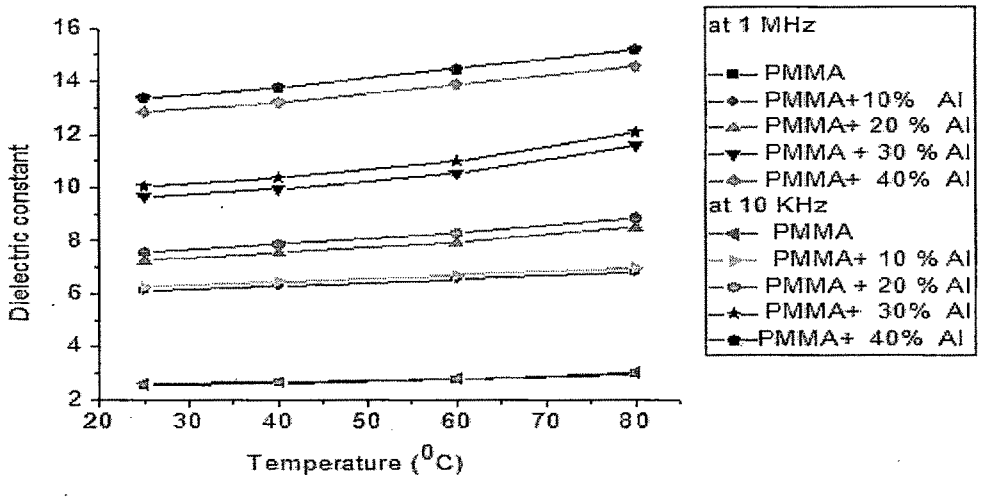

Fig. 3.19 Variation of dielectric constant vs temperature with different concentrations of PMMA/Al composites at two different frequencies.

(e) Frequency dependence dielectric loss

Figure 3.20 (a-c) shows the variation of dielectric loss with frequency, filler concentration and ion fluence for PMMA/Al composites. The dielectric loss decreases exponentially and then became less dependent on frequency. This is because the

induced charges gradually fail to follow the reversing field causing a reduction in the electronic oscillations as the frequency is increased [22,23].

(f) Temperature dependence dielectric loss

Figure 3.21 shows the plot of dielectric loss versus frequency at different concentrations and temperatures. Figure 3.22 shows the plot of dielectric loss versus temperature for different concentrations of the composites at the frequencies of 10 kHz and 1 MHz. It is observed that dielectric loss increases as temperature increases. The dielectric loss is due to the perturbation of phonon system by an electric field, the energy transferred to the phonon is dissipated in the form of heat. The increase in dielectric loss with increasing filler contents may be attributed to the interfacial polarization mechanism of the heterogeneous system.

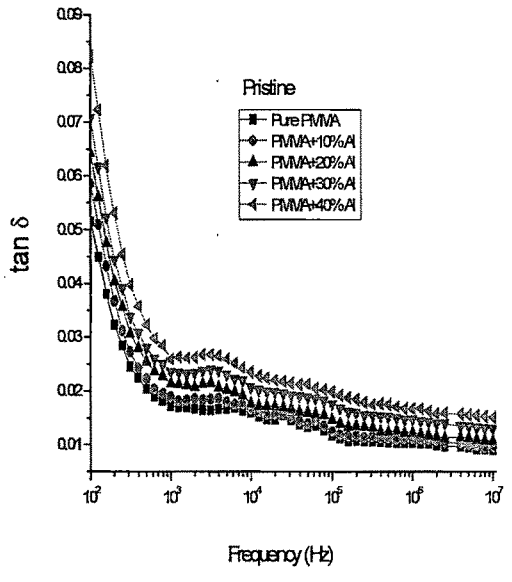

(a)

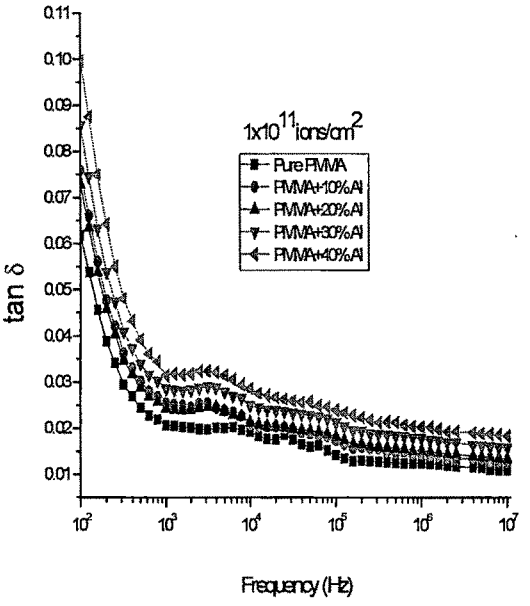

(b)

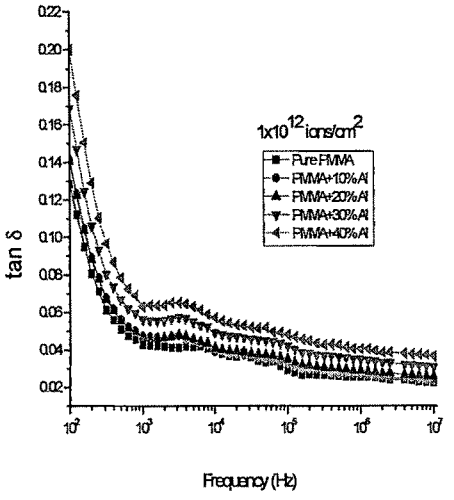

(c)

Fig.3.20 Dielectric loss vs. frequency for PMMA/Al composites (a) Pristine and (b) Irradiated at a fluence of $1x10^{11}$ions/cm2 (c) Irradiated at a fluence of $1x10^{12}$ions/cm^2 .

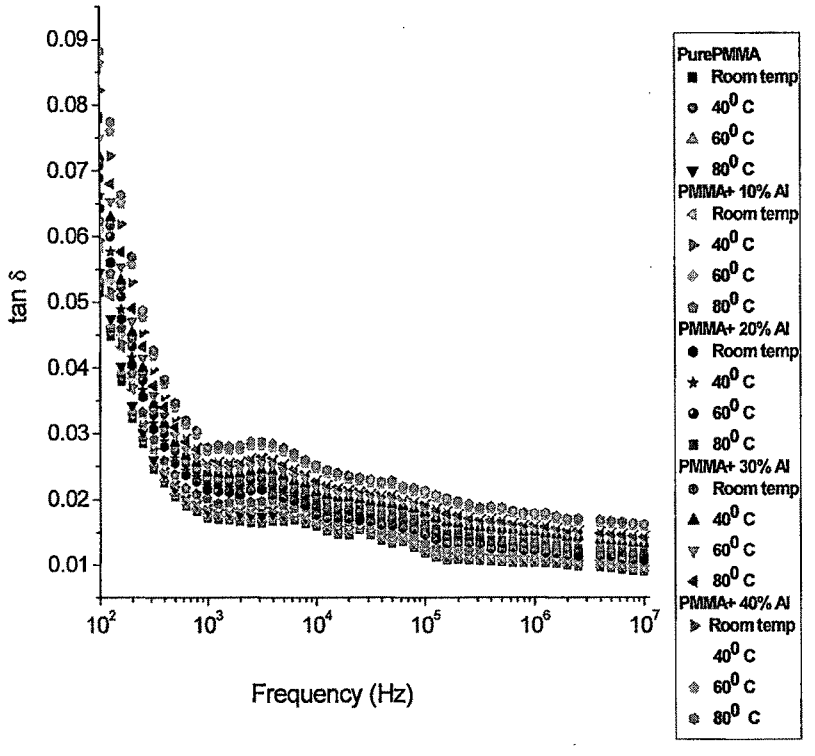

Fig.3.21 Variation of dielectric loss of PMMA/Al composites with frequency of applied electric field, concentration and temperature.

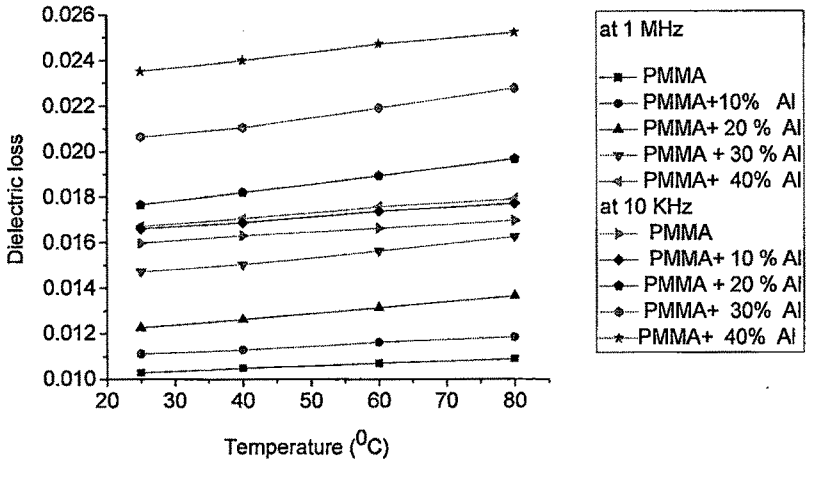

Fig.3.22 Variation of dielectric loss vs temperature at different concentration of PMMA/Al composites at two different frequencies.

3.2.2 X-ray diffraction analysis

Figure 3.23 (a, b) shows the X-ray diffraction patterns of PMMA/Al composites before and after irradiation for 10% and 40 % of Al composites. The peaks are obtained at 2θ = 34.32, 38.19, 39.90 and 44.47. The nature of the peak indicates the semi-crystalline nature of the sample. The crystallite size has been calculated before and after the irradiation using Scherrer's equation [41]

$b = K\lambda/L\cos\theta$

where b is FWHM in radians, λ is the wavelength of X-ray beam (1.5418Å), L is the crystallite size in Å, K is a constant which varies from 0.89 to 1.39, but for most cases it is close to 1. The percentage crystallanity of the composites was determined by area ratio method. In this method the areas of amorphous and crystalline parts of the pattern were calculated. The crystallite size and crystallinity (%) were listed in Table

1. From Fig 3.18 (a, b), the most prominent peaks are approximately obtained around at 2θ ~ 38.19 and 44.47 in all the cases. These peaks are due to pure Al metal (JCPDS) and other peaks are due to aluminum oxide (Al_2O_3) at around 34.32 and 44.47 (JCPDS). It indicates that there is aluminium oxide formation around Al in the composites. The appearance of sharp peak in composite indicates some degree of crystallinity. It was observed that the degree of crystallinity increased upon irradiation of PMMA/Al composites at the fluence of $1x10^{11}$ ions/cm^2 (Table 3.1) for both the composites (i.e 10%, 40%). The crystallinity of polymer composite was decreased on further increase of ion fluence i.e $1x10^{12}$ ions/cm^2 and the polymer composites tend to change into the amorphous phase (Figure 3.23 (a),(b)).

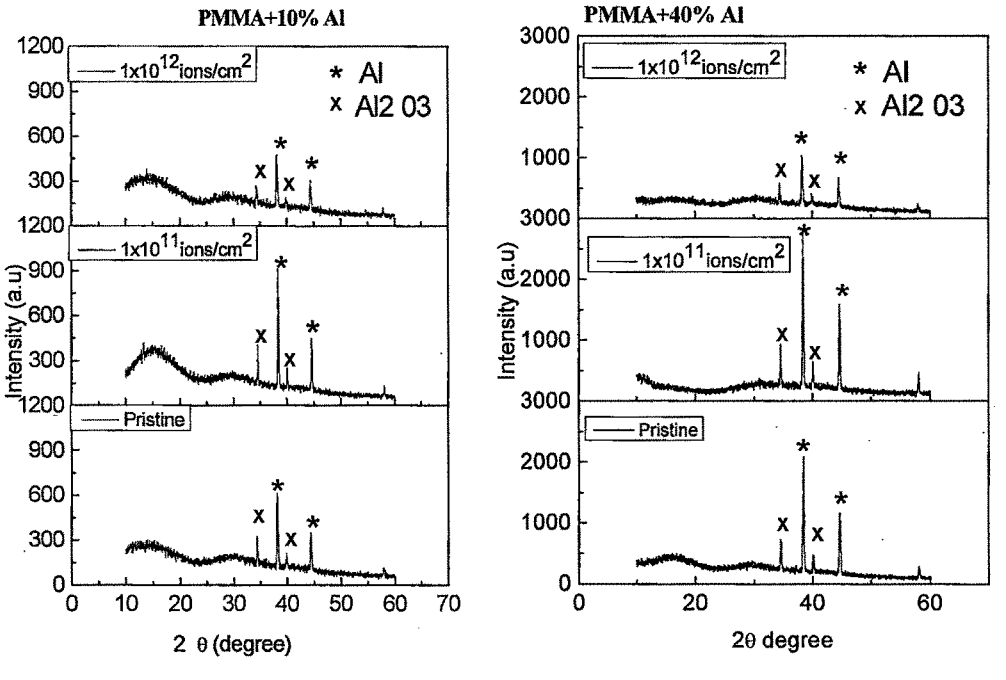

(a) (b)

Fig.3.23 XRD Spectra of (a) PMMA+10%Al (pristine) and PMMA+10%Al (irradiated) at two different fluences of $1x10^{11}$ ions/cm^2 and $1x10^{12}$ ions/cm^2 (b)

PMMA+40%Al (pristine) and PMMA+40%Al (irradiated) at two different fluences of $1x10^{11}$ ions/cm^2 and $1x10^{12}$ ions/cm^2.

Table 3.1

FWHM, crystallite size and % crystallinity of pristine and irradiated PMMA/Al composites for 10% and 40% concentrations of filler.

Pristine (PMMA+10%Al)				**Pristine (PMMA+40%Al)**			
2 theta (deg.)	FWHM (B rad.)	Crystallite Size (nm)	Crystallinity (%)	2 theta (deg.)	FWHM (B rad.)	Crystallite Size (nm)	Crystallinity (%)
34.32	0.3032	30.8	1.62	34.53	0.2642	35.0	4.170
38.19	0.3065	30.6	5.61	38.40	0.2632	35.56	16.65
39.90	0.3146	30.9	0.95	40.11	0.2512	37.41	2.431
44.47	0.3196	29.4	3.05	44.65	0.2912	32.83	10.10
Average Crystallite Size = 30.35 nm Average Crystallinity = 2.81 %				Average Crystallite Size = 35.20 nm Average Crystallinity = 8.34 %			
1x 10^{11}ions/cm^2 (PMMA+10% Al)				**1x 10^{11}ions/cm^2 (PMMA+40%Al)**			
2 theta (deg.)	FWHM (B rad.)	Crystallite Size (nm)	Crystallinity (%)	2 theta (deg.)	FWHM (B rad.)	Crystallite Size (nm)	Crystallinity (%)
34.34	0.249	38.5	2.38	34.49	0.1825	55.65	6.11
38.22	0.2712	35.0	9.27	38.32	0.2158	42.77	32.11
39.92	0.2521	37.5	1.32	40.07	0.1954	48.12	4.11
44.47	0.2962	32.7	3.45	44.60	0.2514	28.18	20.968
Average Crystallite Size = 35.95 nm Average Crystallinity = 4.60%				Average Crystallite Size = 42.51nm Average Crystallinity = 15.82 %			
1x 10^{12}ions/cm^2 (PMMA+10%Al)				**1x 10^{12}ions/cm^2 (PMMA+40%Al)**			

2 theta (deg.)	FWHM (B rad.)	Crystallite Size (nm)	Crystallinity (%)	2 theta (deg.)	FWHM (B rad.)	Crystallite Size (nm)	Crystallinity (%)
34.53	0.2889	32.01	1.54	34.37	0.2063	45.29	1.78
38.36	0.2847	33.47	6.53	38.23	0.2623	35.64	7.94
40.12	0.2617	35.98	0.96	39.93	0.3245	28.94	1.55
44.47	0.2905	32.90	4.16	44.50	0.2854	33. 47	5.41
Average Crystallite Size = 33.59 nm				Average Crystallite Size = 35.8 nm			
Average Crystallinity = 3.29%				Average Crystallinity = 4.17 %			

3.2.3 Differential scanning calorimetric (DSC) analysis

Fig. 3.24 shows DSC thermograms of pristine PMMA, pristine and irradiated PMMA+40%Al composite samples. Tg of the pure PMMA is observed at 69.9 °C and PMMA+40% Al composite pristine and irradiated at fluences of $1x10^{11}$ and $1x10^{12}$ ions/cm^2 are observed at 75.81 °C, 80.71^{0}C and 71.24 °C respectively. As shown in Fig. 3.24, the increase in Tg of composite may be due to the interaction of Al metal particles with PMMA in more ordered state. It is also observed that Tg of composite shifted towards higher temperature at a fluence of $1x10^{11}$ ions/cm^2, which reveals that the composite became more crystalline. On further increase of the fluence (ie. $1x10^{12}$ions/cm^2) , Tg shifted to lower temperature, which reveals that the irradiation leads to chain scission and subsequently reduction in molecular weight. As a result, the system is changing towards disordered state. It is also confirmed with XRD results.

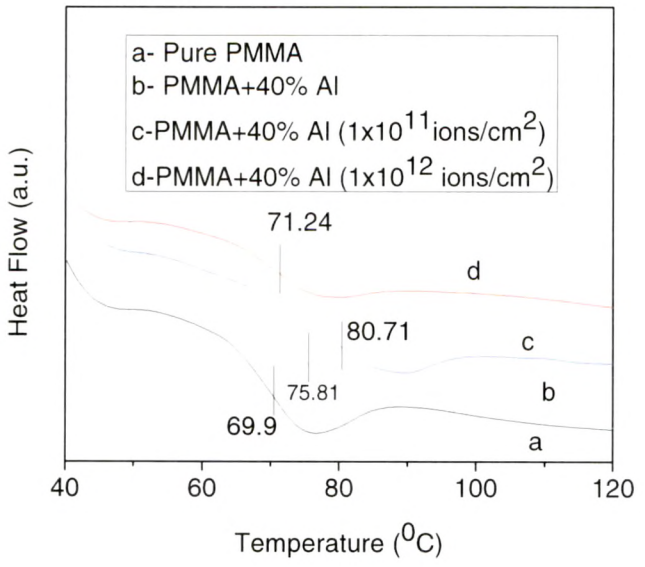

Fig. 3.24 DSC thermograms of (a) pure PMMA pristine, (b) PMMA+40% Al (pristine) and (c) PMMA+40% Al (irradiated at a fluence of $1x10^{11}$ions/cm^2) (d) PMMA+40% Al (irradiated at a fluence of $1x10^{12}$ions/cm^2).

3.2.4 Surface morphology

(i) Atomic force microscopy (AFM) analysis

The surface morphology of pristine and irradiated films of PMMA/Al composites (10% and 40 %) was studied by AFM on 5×5 μm^2 area and shown in Fig. 3.25 (a-d). Each AFM image was analyzed in terms of surface average roughness (Ra). The surface average roughness values obtained are 1.7 and 8.2 nm for 10% and 40% Al dispersed PMMA composites respectively before irradiation. The roughness values of correspondingly irradiated (at a fluence of $1x10^{12}$ ions/cm^2) samples are 4.3 and 13.4 nm respectively. It is found that

roughness increases as filler concentration increases. The increase in roughness may be due to the increase of density and size of metal particles on the surface of the

PMMA films [32]. Ion irradiation of polymers leads, in general, to an increase in surface roughness due to large sputtering effects.

(ii) Scanning electron microscopy (SEM) analysis

The scanning electron microscopy (SEM) images were taken for pristine and irradiated samples of 10% and 40% Al metal dispersed PMMA composites. The significant change in surface topography was observed with filler concentration and also upon irradiation. Fig. 3.27(a-d) shows SEM images of pristine and irradiated composites. It can be seen that the connectivity of the polymer metal phase increases with increasing metal content in polymer matrix as would be expected from conductivity results. As the aluminum content is increased (i.e. 40% Al filler), the continuous chains consisting of Al particles are seen. It means the metal particles are in contact to each other (Fig. 3.26(c)). The metal polymer phases are increased due to ion beam irradiation as shown in Fig.3.26(b) and 3.26(d).

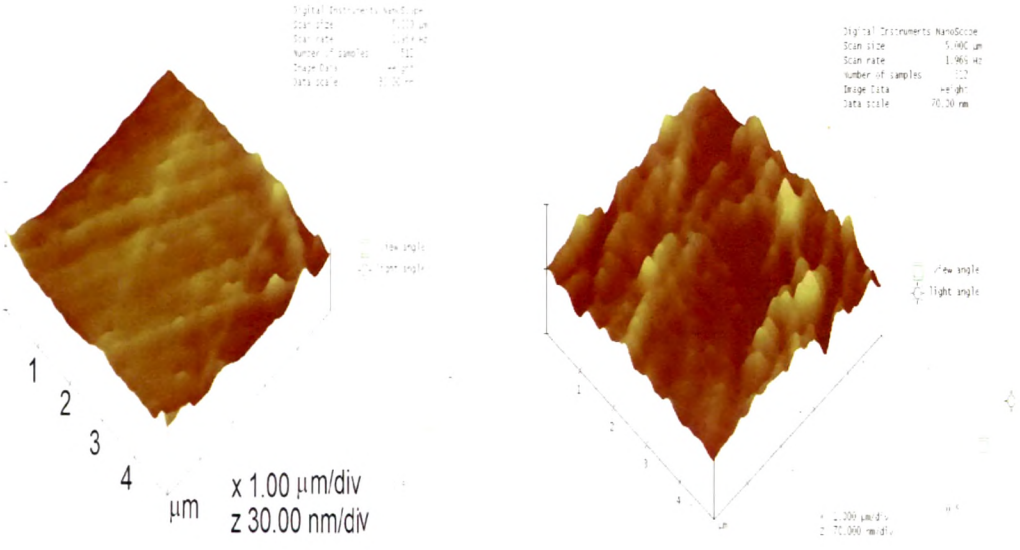

(a) (b)

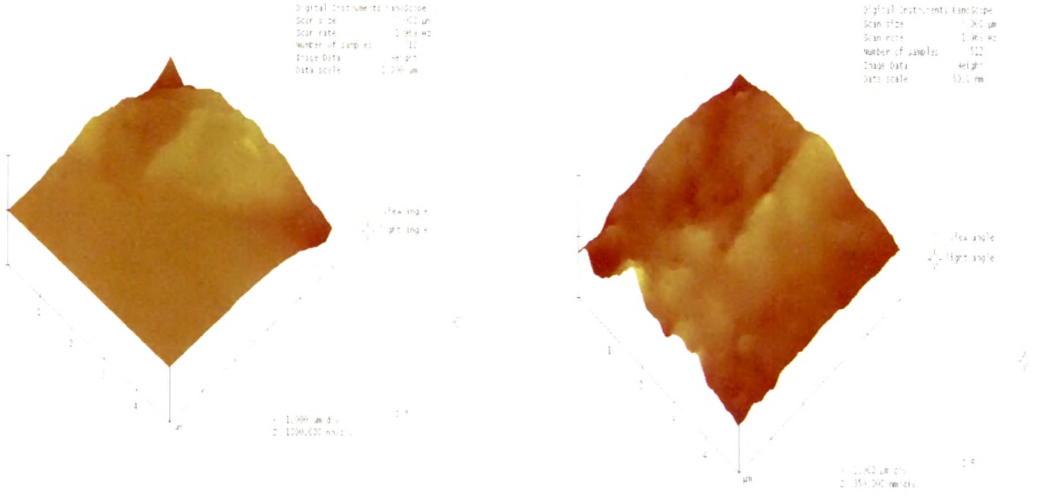

(c) (d)

Fig. 3.25 AFM images of PMMA+10% Al (a) pristine (b) at 1×10^{12} ions/cm^2 and PMMA+40% Al (c) pristine (d) at 1×10^{12} ions/cm^2.

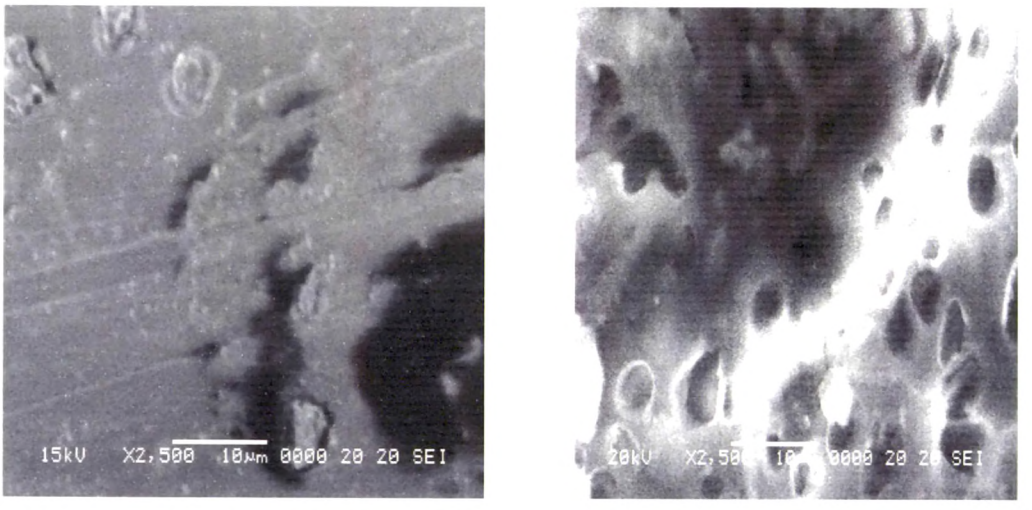

(a) (b)

(c)

(d)

Fig. 3.26 SEM images of PMMA+10% Al (a) pristine (b) at 1 × 10^{12} ions/cm^2 and PMMA+40% Al (c) pristine (d) at 1 × 10^{12} ions/cm^2.

3.3. 6 Conclusions

(1) Both dielectric constant and dielectric loss of Al/PMMA composites increased with an increase in concentration of aluminium, which are attributed to interfacial polarization of heterogeneous system. Both dielectric constant and dielectric loss of Al/PMMA composites decreased with an increase in frequency.

(2) The dielectric constant of the Al/PMMA composites increased with an increase in temperature, which are attributed to the segmental mobility of the polymer molecules.

(3) The study of ac conductivity depends on the frequency allowed us to identify different mechanisms of the conduction in the Al/PMMA composites. At low frequencies, the conductivity is dominated by a percolative behavior, and at higher frequencies it obeys the Jonscher power law. Ac electrical conductivity and dielectric properties of the composites increased after ion beam irradiation due to chain scissoning phenomena occurring in polymer composites.

(4) X-ray diffraction spectrum shows the semicrystalline nature of the PMMA/Al composites. Percentage crystallinity of the composites increases at low fluence and then decreases at higher fluence. It means that the composite system is moving towards the crystalline state at low fluence and tends to change towards disordered state at higer ion fluence.

(5) Thermal property of the composite was studied by DSC analysis and it reveals that the Tg shifted towards higher temperature at low fluence and then shifted towards lower temperature on further increase of fluence. It means that the composite system is moving towards the crystalline state at low fluence and tends to change towards disordered state (amorphous) at higher ion fluence. XRD analysis also supports these results.

(6) The surface roughness increases as Al particle concentration increases and also with ion beam irradiation as observed from AFM analysis. The contact of the particles increased on increasing the concentration of filler and connectivity further increases upon irradiation as revealed from SEM analysis, it is also confirmed by conductivity results.

3.3. Copper filled PMMA composites: Results and discussion

3.3.1 Electrical properties

(a) Frequency dependence ac conductivity

Fig. 3.27 (a-d) shows the conductivity of PMMA/Cu composites with frequency of applied electric field, filler concentration and fluence. It is observed that the conductivity increases gradually with frequency for pure PMMA and 10% Cu composite, while for higher filler concentration conductivity is observed to be frequency independent upto 1MHz and then shows strong dependence on it. At low frequencies, the conductivity of these composites remains constant, this is due to dc

contribution (σ_{dc}), when the frequency is increased the ac-conductivity is found to obey a power law ($\sigma_{ac}=Af^{n}$). As shown in figure 3.27(a-c), 0 % and 10% composites behave as an insulating phase and after further doping at higher concentrations (i.e.20%, 30% and 40%), samples show conductive behavior [38]. Fig. 3.27(d) shows the dependence of conductivity on filler concentration at a frequency of 1MHz. The conductivity also increases upon irradiation. This increment in conductivity upon irradiation is probably due to the production of large number of charged and active chemical species, radicals and electrons along the ion track [25].

(b)Temperature dependence ac conductivity

It is observed that the conductivity increases with increasing temperature, frequency and filler content as shown in Fig 3.28 for all pristine composites. It was found that AC conductivity increases with increasing temperature due to thermal activation or it is due to the tremendous increase of the mobility of charge carriers in the composites [42].

Figure 3.29 shows the variation of ln (Ac-conductivity) with the inverse temperature for all pristine samples at two fixed frequencies (1 MHz and 10 MHz). The conductivity increased with increasing temperature and this behavior can be explained by suggesting that the electronic charge must hop between metal particles.

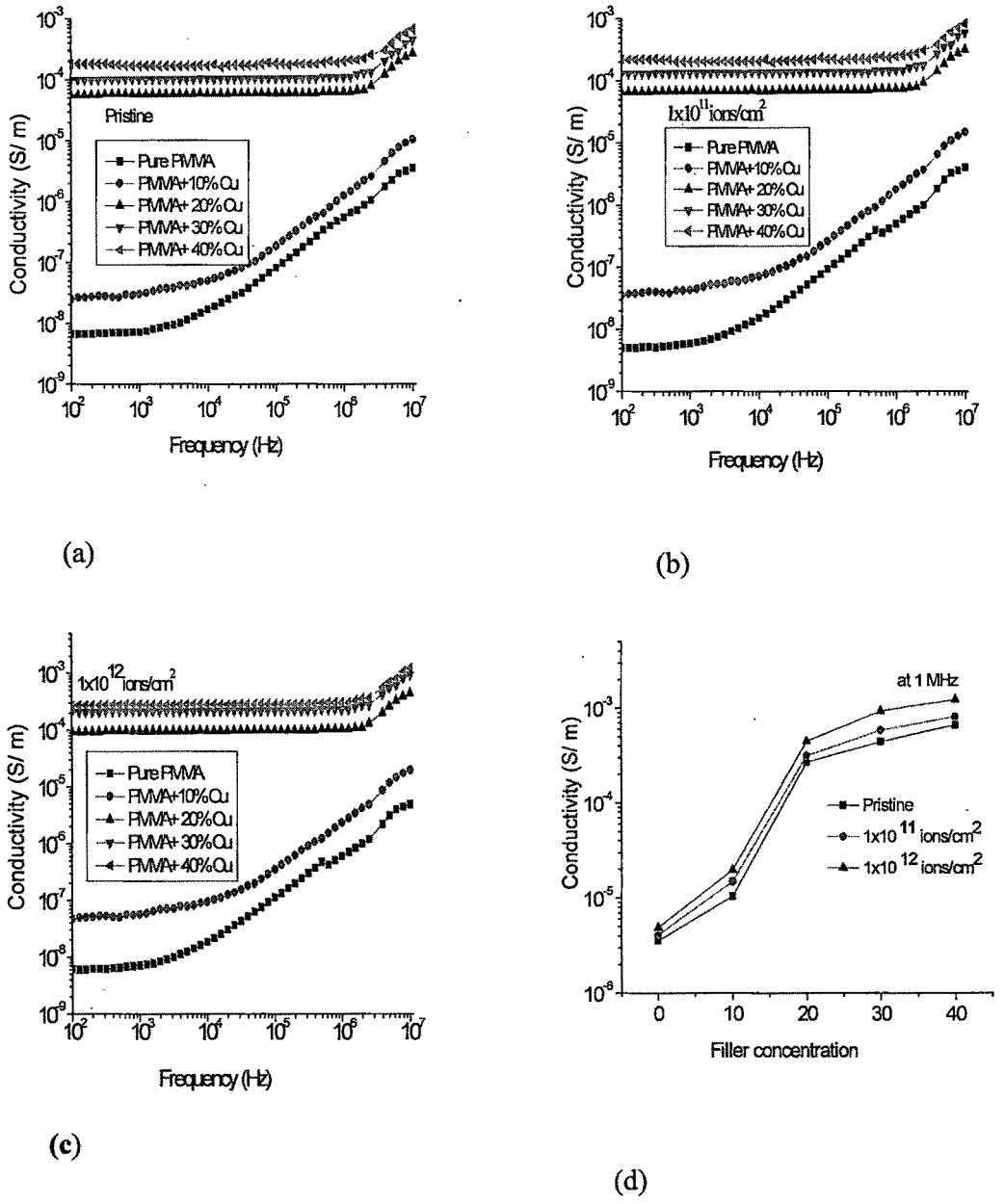

Fig. 3.27 Conductivity vs. frequency for PMMA/Cu composites (a) Pristine and (b) Irradiated at a fluence of $1x10^{11}$ions/cm^2 (c) Irradiated at a fluence of $1x10^{12}$ions/cm^2 (d) Conductivity vs. filler concentration at 1MHz.

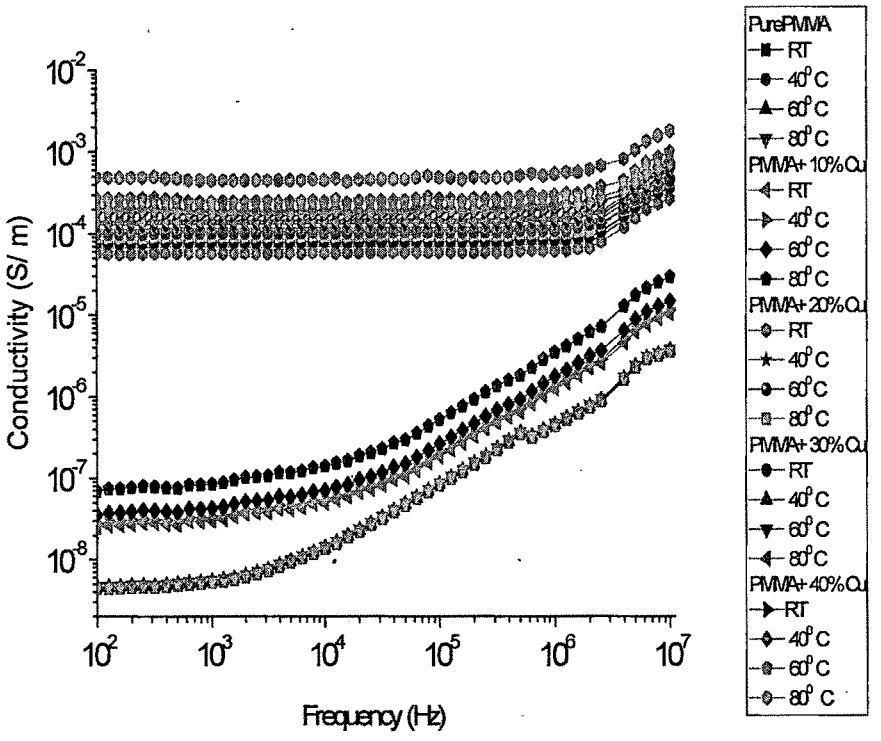

Fig.3.28 Variation of conductivity of PMMA/Cu composites with frequency of applied electric field, concentration and temperature.

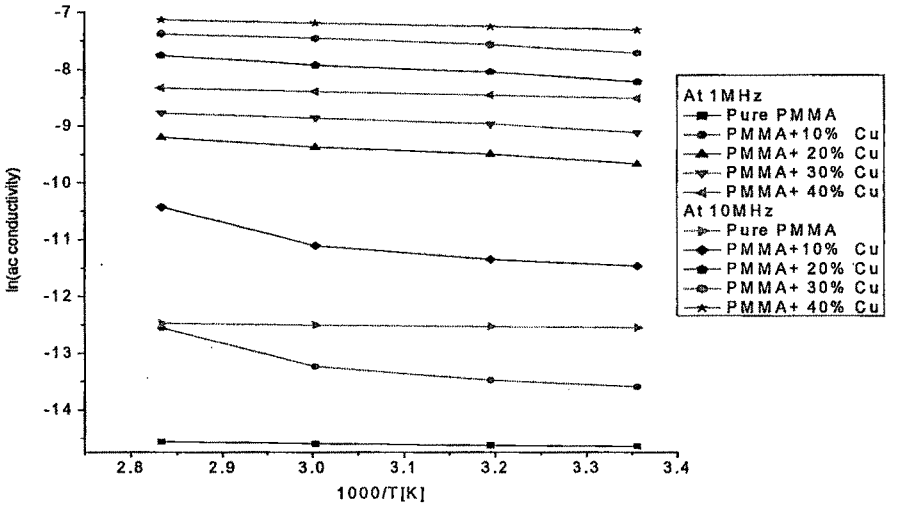

Fig.3.29 Plot of natural log of conductivity (lnσ) versus inverse temperature, 1000/T [K] for PMMA/Cu composites.

(c) Frequency dependence dielectric properties

Fig.3.30 (a-c) shows the variation of dielectric constant of PMMA/Cu composites as a function of frequency at different concentrations of Cu filler and at different fluences of Ag $^{11+}$ ions (140 MeV). For a pure PMMA film, the dielectric constant is 2.5 at a frequency of 1 MHz. After inserting 10% Cu particles in polymer matrix, the dielectric constant increased to 8.8. It was observed that the dielectric constant increases with increasing the concentration of the copper. Similar results were also observed by the number of researchers [43-46]. The dielectric constant was found to increase further upon SHI irradiation. The increase in dielectric constant of irradiated samples may be attributed to the disordering of the material by means of chain scission in polymer composites. Radicals or dangling bonds are created by the release of pendant atoms such as hydrogen. Cross-linking occurs when two dangling bonds on neighbouring chains unite [47, 48].

(d)Temperature dependence dielectric properties

Figure 3.31 shows the variation of dielectric permittivity of polymer composites with frequency of applied electric field, concentration of filler and temperature. Fig.3.32 shows the variation of dielectric constant with temperature. It can be seen that the dielectric constant increases on increasing temperature and moderately decreases with increasing applied electric field frequency. The dielectric constant of the PMMA/Cu composites increased with an increase in temperature, which has been attributed to the segmental mobility of the polymer molecules [26].

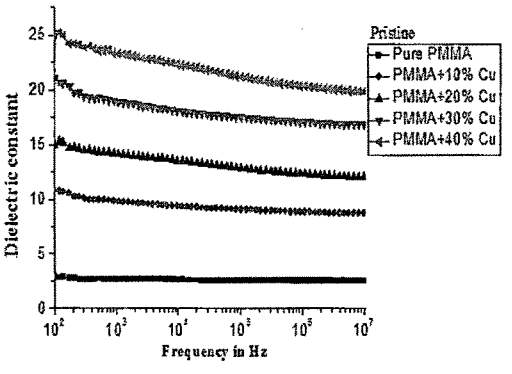

(a)

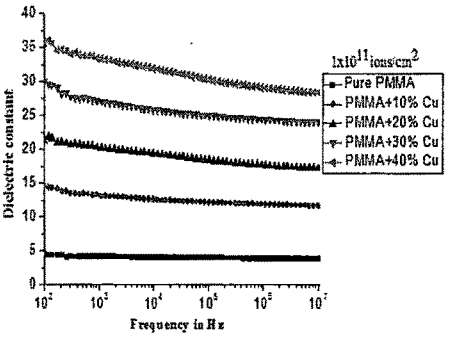

(b)

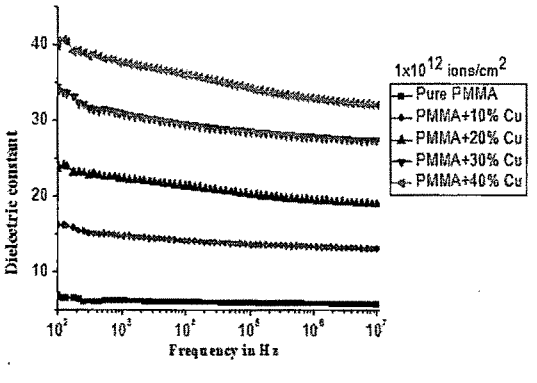

(c)

Fig.3.30 Dielectric constant vs. frequency for PMMA/Cu composites (a) Pristine and (b) Irradiated at a fluence of $1x10^{11}$ions/cm^2 (c) Irradiated at a fluence of $1x10^{12}$ions/cm^2.

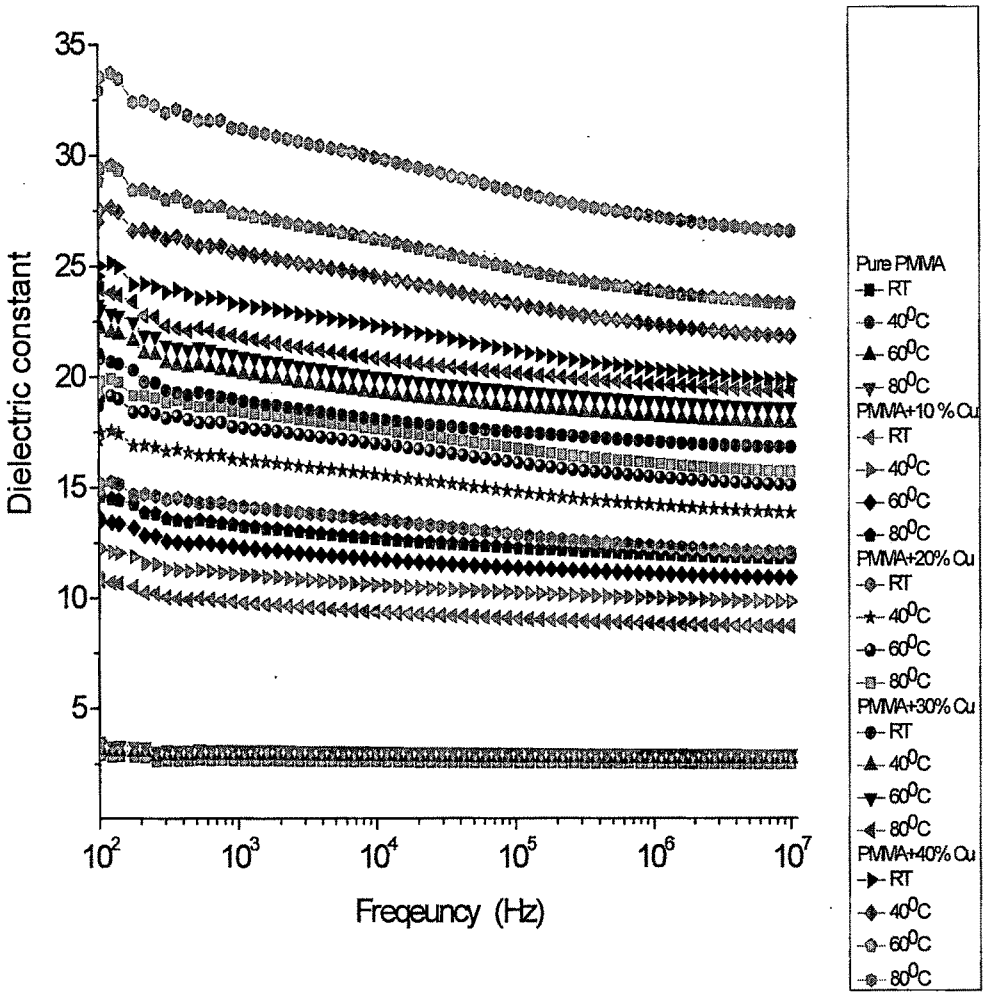

Fig.3.31 Variation of dielectric constant of PMMA/Cu composites with frequency of applied electric field, concentration and temperature.

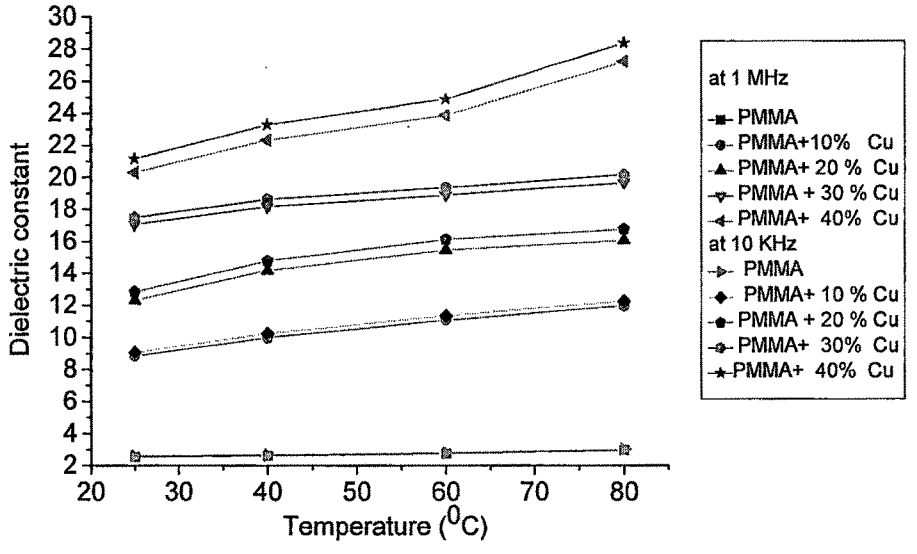

Fig.3.32 Variation of dielectric constant vs temperature at different concentrations of PMMA/Cu composites at two different frequencies.

(e) Frequency dependence dielectric loss

Frequency dependence dielectric loss of the composites as a function of filler concentration and fluence is shown in Fig. 3.33(a-c). The dielectric loss is high at low frequency and as frequency increases, the dielectric loss decreases for all composite samples. It can be seen from figure that as more copper is added to the polymer matrix, dielectric loss, in general, shows an increase. The increase in dielectric loss with the increase in the copper concentration, which is also shown by several other conductor–insulator systems, is considered to be a consequence of interfacial polarization [35]. Dielectric loss also increases moderately upon ion beam irradiation.

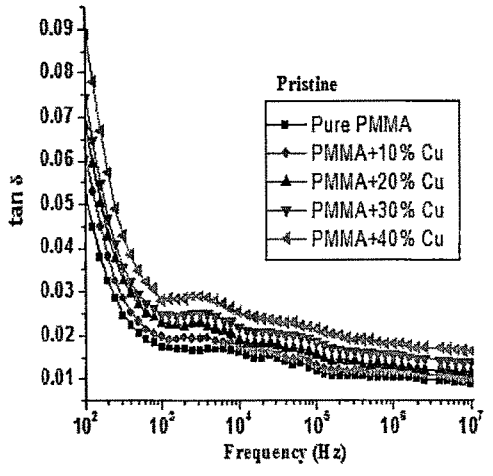

(a)

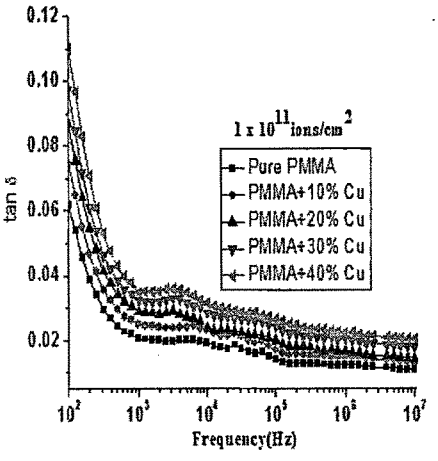

(b)

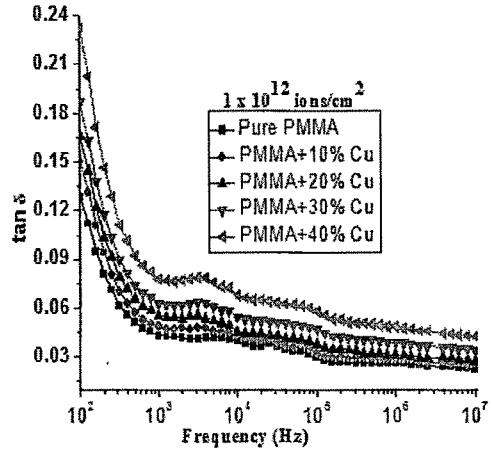

(c)

Fig.3.33 Dielectric loss vs. frequency for PMMA/Cu composites (a) Pristine and (b) Irradiated at a fluence of $1x10^{11}$ions/cm^2 (c) Irradiated at a fluence of $1x10^{12}$ions/cm^2 .

(e) Temperature dependence dielectric loss

Figure 3.34 shows the variation of dielectric loss versus frequency at different concentrations and different temperatures for pristine PMMA/Cu composites. Figure 3.35 shows the plot of dielectric loss versus temperature for different concentrations of the composites at the frequencies of 10 kHz and 1 MHz. Dielectric loss increases with increasing temperature. The dielectric loss is due to the perturbation of phonon system by an electric field, the energy transferred to the phonon is dissipated in the form of heat.

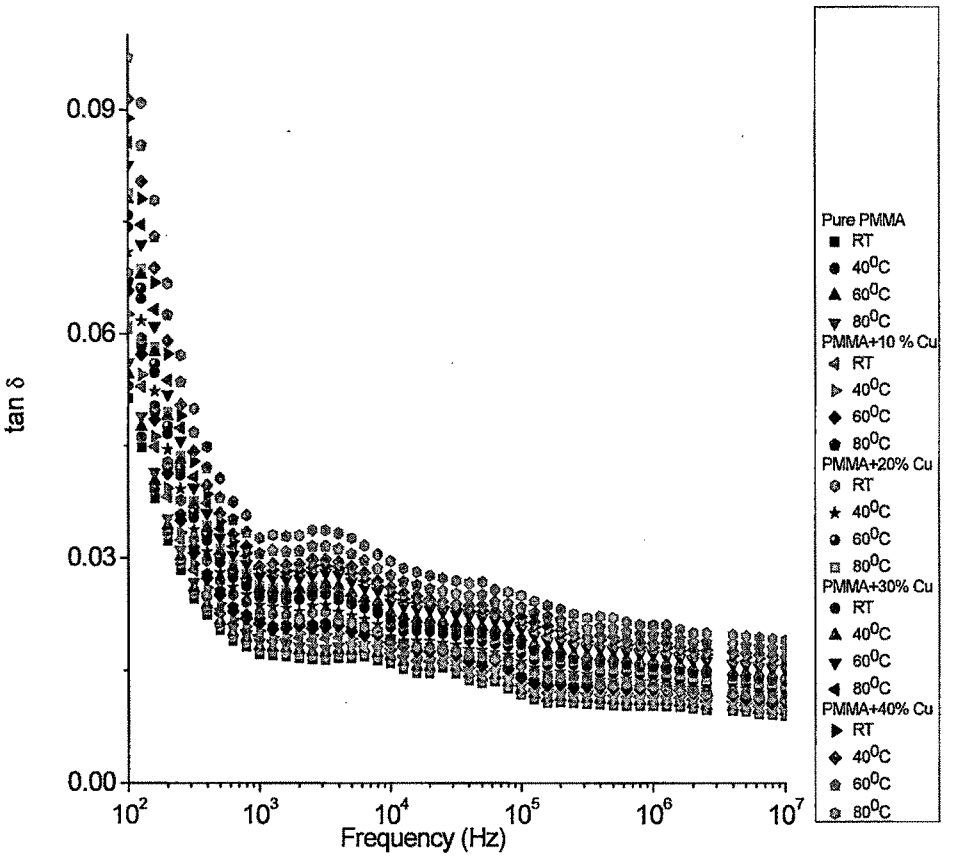

Fig. 3.34 Variation of dielectric loss of PMMA/Cu composites with frequency of applied electric field, concentration and temperature.

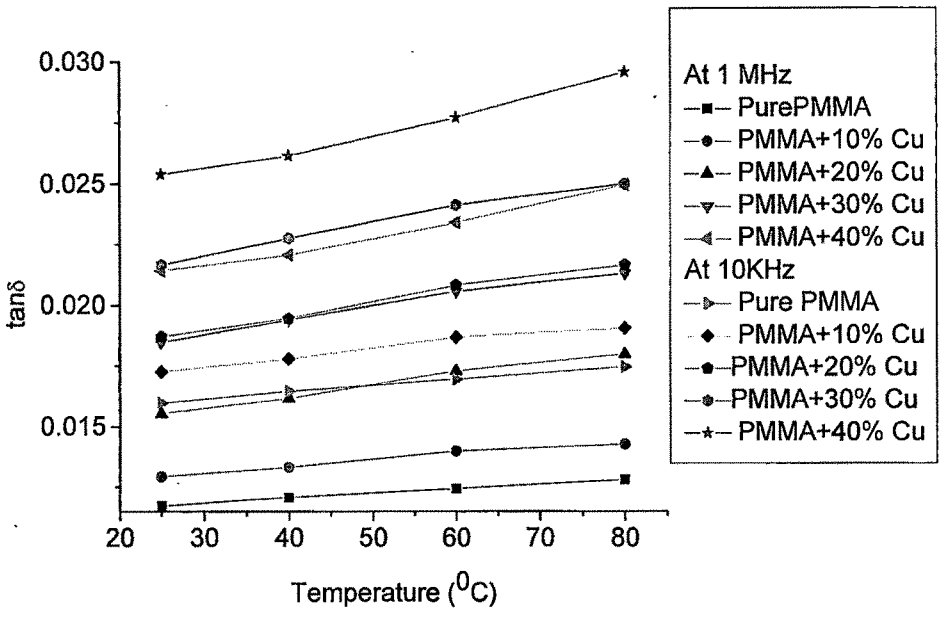

Fig. 3.35 Variation of dielectric loss vs temperature at different concentrations of PMMA/Cu composites at two different frequencies.

3.3.2 X-ray diffraction analysis

Fig. 3.36(a) shows the spectra of pure PMMA, which is amorphous in nature. Fig. 3.36 (b, c) represents the PMMA/Cu composites (for 10% and 40% Cu) before and after SHI irradiation at different fluences. The peaks are obtained at 2θ = 38.92, 43.28, 45.26 and 50.43 in all the cases. The nature of peaks indicates the semi crystalline nature of the samples.

The most prominent peaks are observed around 2θ = 43.28 and 50.43 in all cases. These peaks are due to pure Cu metal (JCPDS: 85-1326) and another peaks are due to copper oxide (CuO) at around 38.92 and 45.26 (JCPDS: 80-0076). It means that the composite materials are accompanied by an inter phase of CuO between polymer matrix and Cu-filler.

The X- ray diffraction patterns indicate that the intensity of diffraction peaks of PMMA/Cu composites increases gradually at low fluence ($1x10^{11}$ ions/cm^2) but

decreases on further increase of the fluence (i.e $1x10^{12}$ ions/cm^2) for both composite samples, Fig. 3.36(b, c). The increase in intensity at low fluence means that the sample became crystalline at low fluence but on further increase of the fluence, the intensity of the diffraction peaks decreased and broadened and tends towards the amorphisation at higher fluence due to increase of unsaturation, free radicals etc. The crystallite size has been calculated before and after the irradiation using Scherrer's equation [41]

$b = K\lambda/L\cos\theta$

where b is FWHM in radians, λ is the wavelength of X-ray beam (1.5418Å), L is the crystallite size in Å, K is a constant which varies from 0.89 to 1.39, but for most cases it is close to 1. The percentage crystallanity of the composites was determined by area ratio method. In this method the areas of amorphous and crystalline parts of the pattern were calculated. The average crystallite size and crystallinity (%) are listed in Table 3.2. The appearance of sharp peak in composite indicates some degree of crystallinity and the degree of crystallinity increases upon irradiation of PMMA/Cu composite at a fluence of $1x10^{11}$ ions/cm^2 (Table 2) for both composites (i.e 10%, 40%). Interaction of ion beam with composite resulted in the formation of gaseous products accompanied by cross-linking i.e. formation of intermolecular bonds at the fluence of $1x10^{11}$ ions/cm^2.On further increase of the fluence, irradiation induced large amount of energy deposition in the composite and leads to decrease in crystallite size, which may be attributed to splitting of crystalline grains [49].

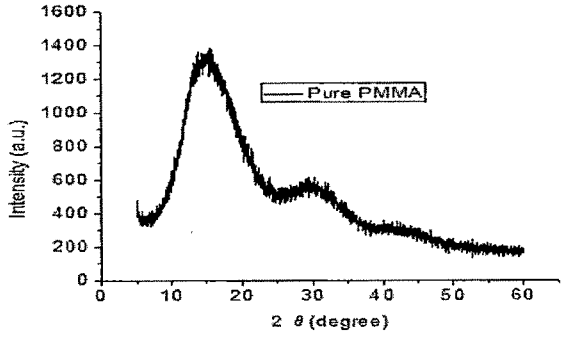

(a)

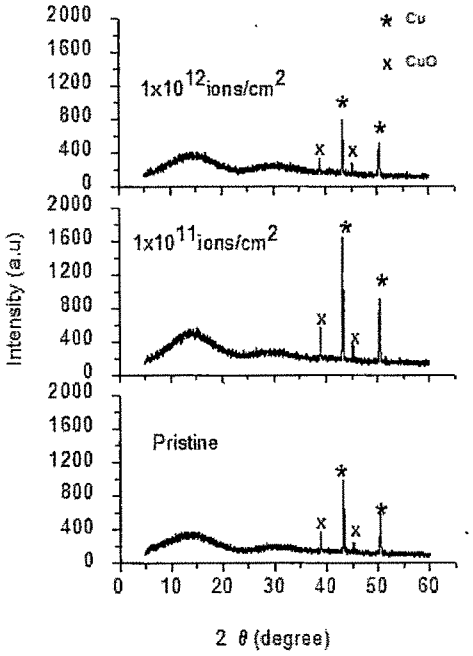

(b)

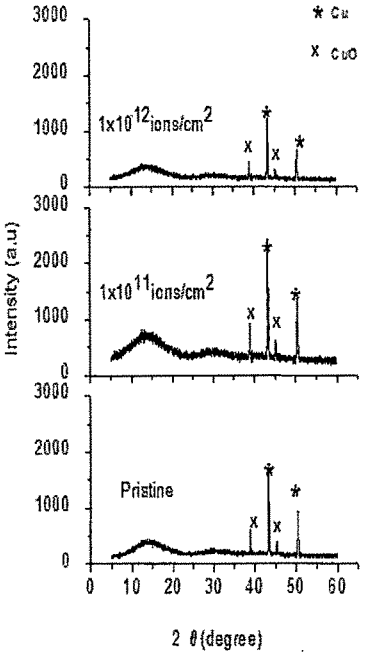

(c)

Fig.3.36 XRD spectra of (a) Pure PMMA (b) PMMA+10% Cu of pristine and irradiated samples. (c) PMMA+40% Cu of pristine and irradiated samples.

Table 3.2

FWHM, crystallite size and % crystallinity of pristine and irradiated Cu/PMMA composites for 10% and 40% concentration of filler.

Pristine (PMMA+10% Cu)				**Pristine (PMMA+40% Cu)**			
2 theta (deg.)	FWHM (B rad.)	Crystallite Size (nm)	Crystallinity (%)	2 theta (deg.)	FWHM (B rad.)	Crystallite Size (nm)	Crystallinity (%)
38.928	0.2032	46.08	1.24	38.914	0.1670	57.03	1.67
43.282	0.2029	46.82	6.35	43.262	0.1854	51.33	16.26
45.261	0.2195	43.57	0.88	45.239	0.1859	45.29	2.71
50.437	0.2861	34.10	4.71	50.396	0.2612	37.56	7.19
Average Crystallite Size = 42. 64 ± 5.86 nm				Average Crystallite Size = 47.80 ± 8.34nm			
Average Crystallinity = 3.29 ± 2.67%				Average Crystallinity = 7.0 ± 6.64%			
1x 10^{11}ions/cm^2 (PMMA+10% Cu)				**1x 10^{11}ions/cm^2 (PMMA+40% Cu)**			
2 theta (deg.)	FWHM (B rad.)	Crystallite Size (nm)	Crystallinity (%)	2 theta (deg.)	FWHM (B rad.)	Crystallite Size (nm)	Crystallinity (%)
38.90	0.1728	54.18	7.7	38.820	0.1733	55.0	1.94
43.259	0.1899	50.00	5.6	43.165	0.1890	50.32	8.86
45.231	0.2019	47.3	2.5	45.157	0.1893	50.65	1.07
50.38	0.2743	35.5	1.13	50.306	0.2595	37.65	6.22
Average Crystallite Size = 46.78 ± 8.01nm				Average Crystallite Size = 48.40 ± 7.48nm			
Average Crystallinity = 4.32 ± 2.91%				Average Crystallinity = 9.82 ± 3.73%			

1x 10^{12}ions/cm^2 (PMMA+10% Cu)				1x 10^{12}ions/cm^2 (PMMA+40% Cu)			
2 theta (deg.)	FWHM (B rad.)	Crystallite Size (nm)	Crystallinity (%)	2 theta (deg.)	FWHM (B rad.)	Crystallite Size (nm)	Crystallinity (%)
38.89	0.1968	47.57	4.63	38.877	0.1745	53.65	1.57
43.28	0.2365	24.09	3.26	43.227	0.2072	46.66	7.87
45.23	0.2176	43.9	0.77	45.210	0.1943	49.67	0.82
50.40	0.278	35.10	0.58	50.378	0.2738	35.81	5.22
Average Crystallite Size = 37.66 ± 10.45nm				Average Crystallite Size = 46.32 ± 7.64nm			
Average Crystallinity = 2.31 ± 1.97%				Average Crystallinity = 3.87 ±3.28 %			

3.3.3 Differential Scanning calorimetric (DSC) analysis

Considering the thermal properties of the composites, we must point out the important property of the glass transition temperature (Tg) of polymer. This is defined as the temperature where the plastic becomes hard and brittle when cooled rapidly after heating. At the glass transition temperature, the weak secondary bonds that stick the polymer chains are broken, and the macromolecule starts to move. Fig. 3.37 shows DSC thermograms of pristine PMMA, pristine and irradiated PMMA+40%Cu composite samples. Tg of the pure PMMA is observed at 72.9 °C and PMMA+40% Cu composite pristine and irradiated at fluences of $1x10^{11}$ and $1x10^{12}$ ions/cm^2 are observed at 95.9 °C, 98.5°C and 93.5 °C respectively.

As shown in Fig. 3.37, the increase in Tg of composite may be due to the interaction of Cu metal particles with PMMA in more ordered state [50]. It is also observed that Tg of composite shifted towards higher temperature at a fluence of $1x10^{11}$ ions/cm^2,

which reveals that the composite became more crystalline. On further increase of the fluence (ie. $1x10^{12}$ions/cm^2) , Tg shifted to lower temperature, which reveals that the irradiation leads to chain scission and subsequently reduction in molecular weight. As a result, the system is changing towards more disordered state. It is also confirmed with XRD results.

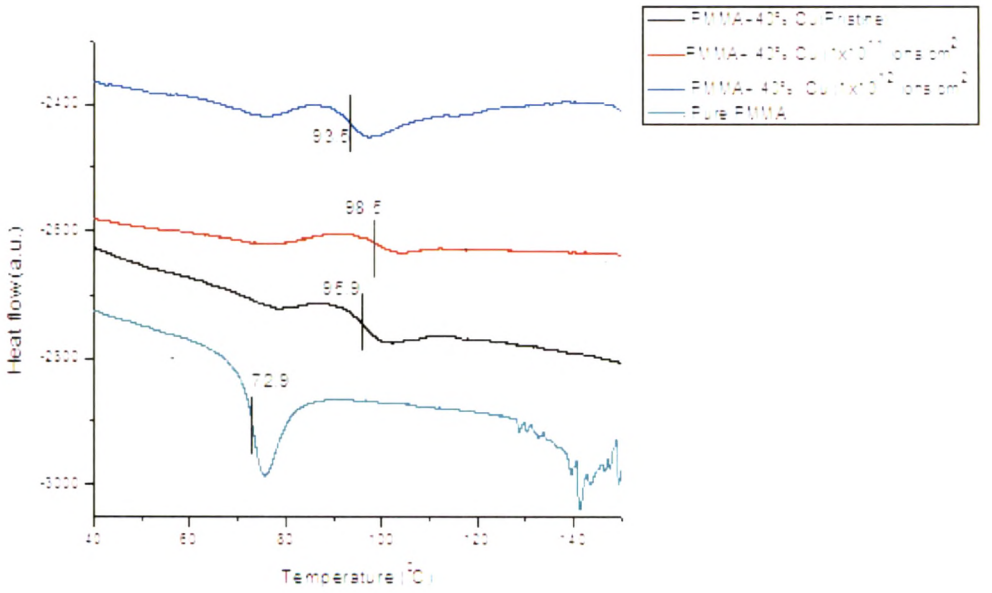

Fig.3.37 DSC thermograms for pure PMMA (pristine) and pristine and irradiated PMMA+40% Cu composites at two different fluences.

3.4.4 Surface morphology

(i) Atomic force microscopy (AFM) analysis

Surface morphology of pristine and irradiated composites was studied using atomic force microscopy in contact mode on 5x5 μm^2 area. The 3-dimensional morphology of pristine and irradiated (at a fluence of $1x10^{12}$ ions/cm^2) samples are shown in figure 3.38(a-d). The average surface roughness values are 0.54 nm and 23.0 nm for pristine composites with filler concentration of 10% and 40% respectively and those of

irradiated samples, the roughness values are 1.53 nm and 31.52 nm respectively. The increase in surface roughness (Ra) with increasing concentration of metal particles may be due to the increase of density and size of metal particles on the surfaces of the polymeric films [32].

(ii) Scanning electron microscopy (SEM) analysis

SEM images are used to examine the texture of the fractured surface of the composites. SEM images were taken for pristine and irradiated samples of 10% and 40% Cu dispersed PMMA composites at 15k X magnification. There are significant changes in surface topography after irradiation. Fig. 3.39 (a-d) shows SEM images of pristine and irradiated composites. It can be seen that the metal particles are isolated at 10% Cu filler i.e. there is no interaction between them (Fig. 3.39a). As the Cu content is increased (i.e. 40% Cu-filler), clusters of metal particles are formed (Fig. 3.39c). A cluster may be considered a region in the polymer matrix, where particles are in physical contact or very close to each other. Aggregates of micro cluster are clearly visible on the surface and metal/polymer phases increase due to ion beam irradiation as shown in Fig. 3.39 (b, d).

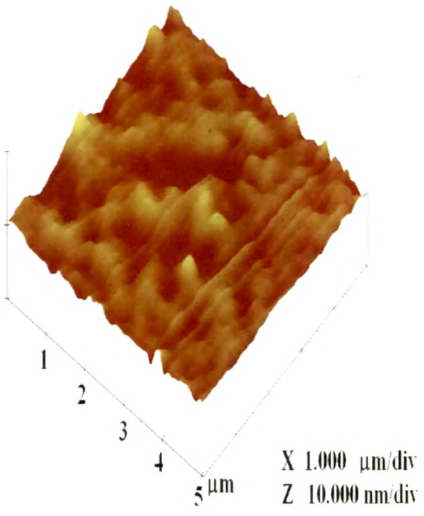

(a)

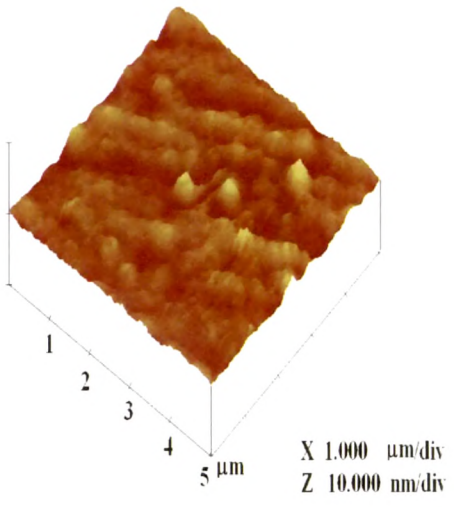

(b)

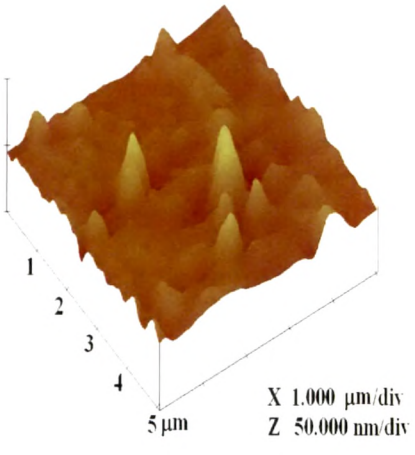

(c)

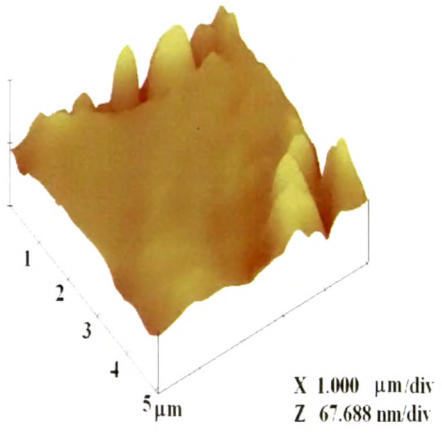

(d)

Fig. 3.38 AFM images of (a) PMMA+10% Cu (pristine) (b) PMMA+10% Cu (fluence 1x10^{12}ions/cm^2). (c) PMMA+40% Cu (pristine) (d) PMMA+40% Cu (fluence 1x10^{12}ions/cm^2).

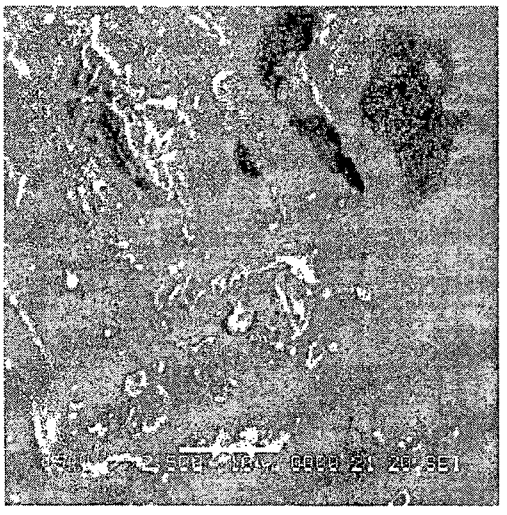

(a)

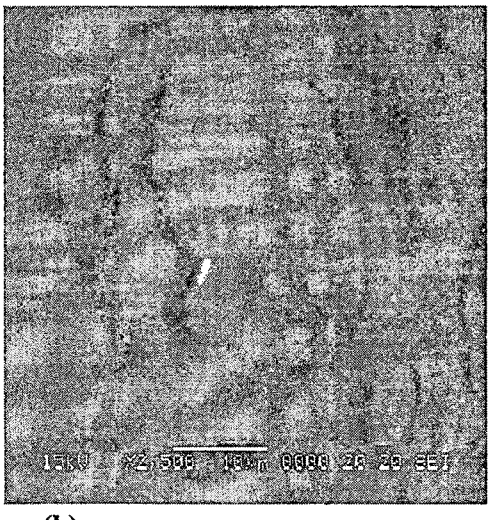

(b)

(c)

(d)

Fig. 3.39 SEM images of (a) PMMA+10% Cu (pristine) (b) PMMA+10% Cu (fluence $1x10^{12}$ions/cm^2). (c) PMMA+40% Cu (pristine) (d) PMMA+40% Cu (fluence $1x10^{12}$ions/cm^2).

3.3.4 Conclusions

The ac conductivity of the composites increases with increasing the frequency, concentration of filler and also with ion fluence. The dielectric constant and dielectric loss are observed to change significantly with filler concentration and also with ion flences. The increase in conductivity and dielectric properties of the composites due to ion beam irradiation may be attributed to (i) metal to polymer bonding and (ii) conversion of the polymeric structure into a hydrogen depleted carbon network due to the emission of hydrogen and/or other volatile gases. Thus irradiation makes the polymer more conductive. The temperature dependence electrical properties were also studied for pristine PMMA/Cu composites. It is observed that ac conductivity, dielectric constant and dielectric loss increased on increasing temperature. The X-ray diffraction patterns of the composites show an increase in crystallinity at lower fluence of $1x10^{11}$ions/cm^2 and decreases on further increase of the fluence. It means polymer composite improved the crystallinity at low fluence and tends to change into the amorphous phase on further increase of the fluence. Thermal property of the composite was studied by DSC analysis and it reveals that the Tg shifted towards higher temperature at low fluence and then shifted towards lower temperature on further increase of the fluence. It means that the composite system is moving towards the crystalline state at low fluence and tends to change towards disordered state (amorphous) at higher ion fluence. XRD analysis also supports these results. The surface roughness increases as filler concentration increases and also with the ion fluence as revealed from AFM studies. SEM micrographs reveal a texture consisting of agglomerates of Cu-particles with particles contact in matrix.

3.4 Summary

Three different fillers dispersed in PMMA polymer matrix and these composites have been irradiated with 140MeV silver ion beam. AC electrical, structural, thermal properties and surface morphology have been investigated using different characterization techniques.

AC electrical conductivity of all pristine and irradiated composites at 40 wt.% filler concentration is shown in Fig. 3.40. AC conductivity behavior is same for all composites but with slightly different magnitude. At low filler concentration (10wt %), the electrical conductivity of the composites increases with increasing frequency. These composites show a typical insulating behavior, i.e frequency-dependent conductivity. When the filler content reaches 20wt%, there is a transition from an insulator to semiconductor. The concentration of the filler, at which composite changes the behavior from insulator to semiconductor is defined as percolation threshold which is associated with the formation of conducting network.

Conductivity is further observed to increase after irradiation in all composites. Irradiation is expected to promote the metal to polymer bonding and convert polymeric structure into hydrogen depleted carbon network. This carbon network is believed to make the polymer more conductive. AC conductivity was studied at different temperature ranging from room temperature to 80^0C for all pristine composites samples and results show that the ac conductivity increases as temperature increases for all cases. Temperature dependence ac electrical conductivity of all pristine composites at 40% filler concentration and at frequency of 10MHz is shown in Fig. 3.41.

Dielectric constant and dielectric loss were studied for all pristine and irradiated composites and results show frequency and fluence dependent behavior for all cases.

In general, the natures of the curves for all samples are same but the magnitude varies with filler material.

The temperature dependence of dielectric constant for all composites can be explained on the basis of two competing mechanisms: segmental mobility of polymer molecules and differential thermal expansion of PMMA and filler particles.

For the sake of comparison, the composites filler content (say 40 wt%) are considered at two different fluences of silver ion beam irradiation (i.e $1x10^{11}$ ions/cm^2 and $1x10^{12}$ions/cm^2) keeping frequency constant (i.e.10 MHz. Similar comparison for dielectric constant and dielectric loss have been considered for all composites and shown in Fig. 3.42 and Fig. 3.43 at a frequency of 10 MHz. Temperature dependence of dielectric constant and dielectric loss of all pristine composites at 40 wt% filler concentration and also at fixed frequency of 10MHz are shown in Figs. 3.44 and 3.45.

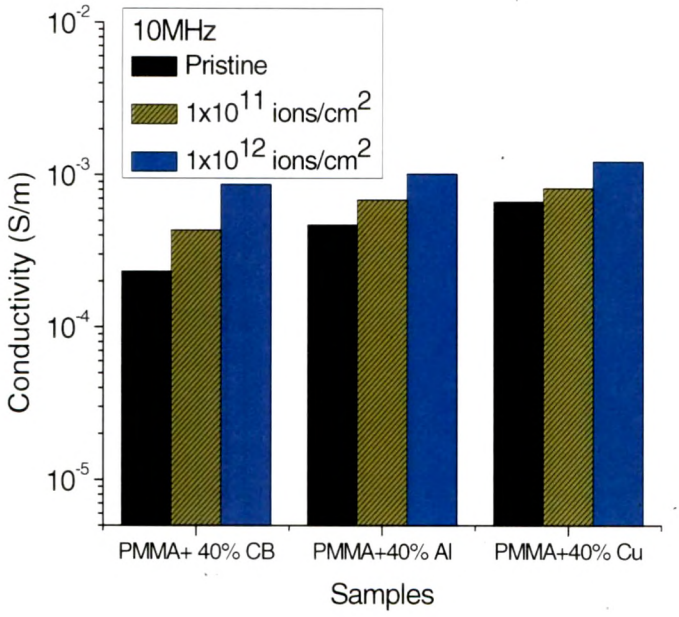

Fig. 3.40 Comparison of conductivity of pristine and irradiated composites at two different fluences (i.e $1x10^{11}$ ions/cm^2 and $1x10^{12}$ ions/cm^2) keeping frequency constant (i.e 10MHz).

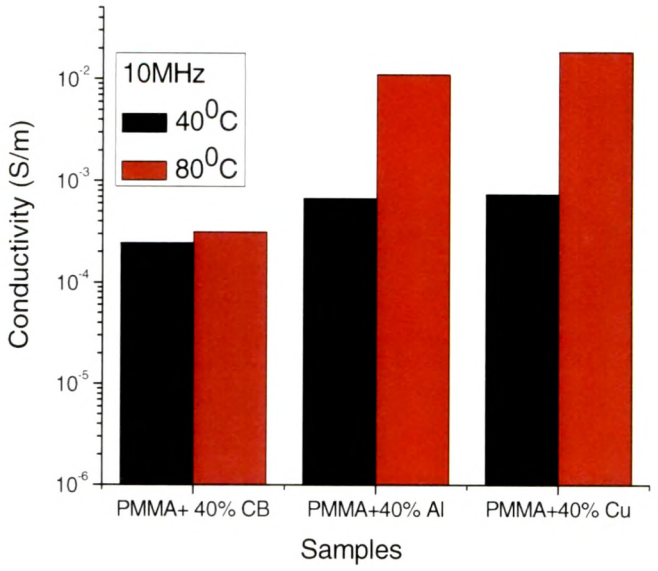

Fig.3.41 Comparison of conductivity of pristine samples for all composites at two different temperatures (40^0C and 80^0C) keeping frequency constant (i.e. 10MHz).

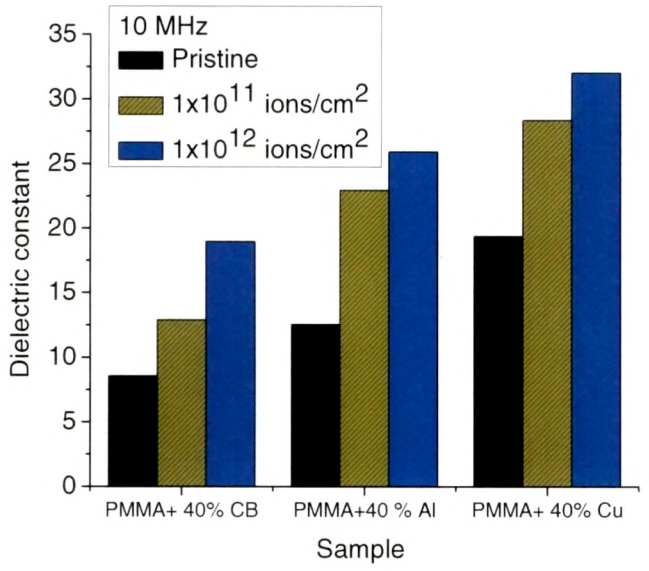

Fig. 3.42 Comparison of dielectric constant of pristine and irradiated composites at two different fluences (i.e $1x10^{11}$ ions/cm^2 and $1x10^{12}$ ions/cm^2) keeping frequency constant (i.e. 10MHz).

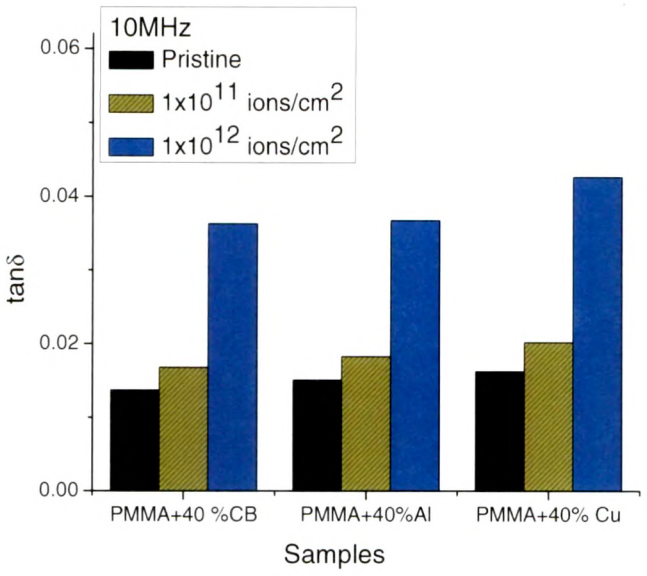

Fig. 3.43 Comparison of dielectric loss of pristine and irradiated composites at two different fluences (i.e $1x10^{11}$ ions/cm^2 and $1x10^{12}$ ions/cm^2) keeping frequency constant (i.e. 10MHz).

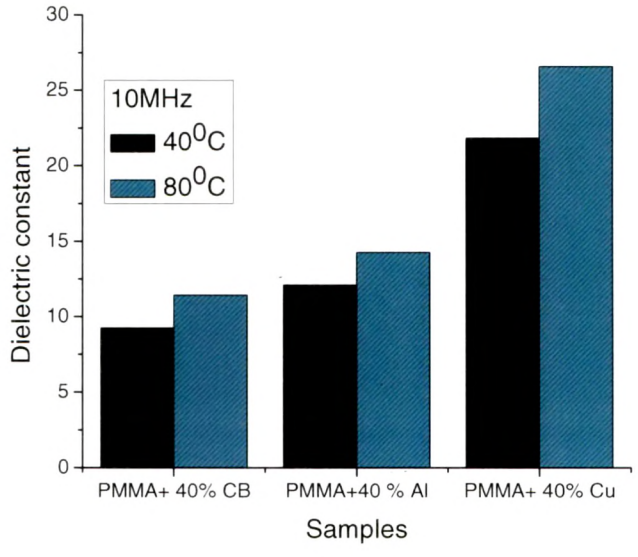

Fig. 3.44 Comparison of conductivity of pristine samples for all composites at two different temperatures (i.e. 40^0C and 80^0C) keeping frequency constant (i.e. 10MHz).

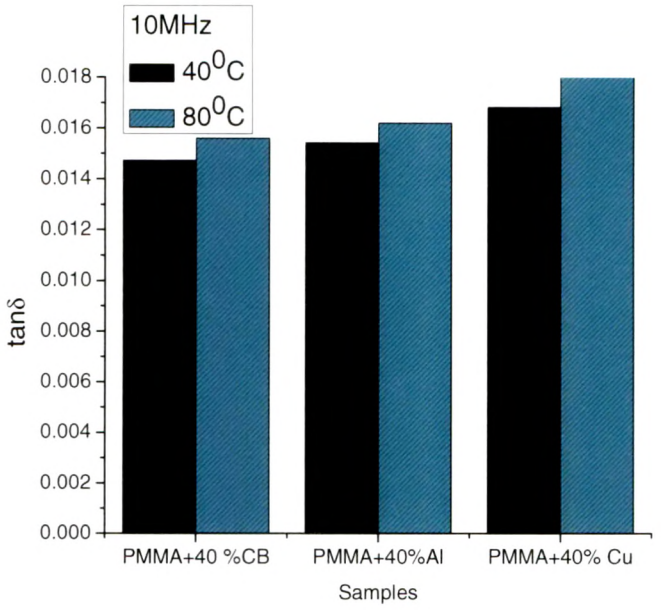

Fig.3.45 Comparison of dielectric loss of pristine samples for all composites at two different temperatures (i.e 40^0C and 80^0C) keeping frequency constant (i.e. 10MHz).

XRD analysis reveals that the pristine and irradiated samples of PMMA/CB exhibit amorphous behavior due to ion beam irradiation where as the XRD results of pristine and irradiated samples of PMMA/Al and PMMA/Cu composites show crystalline nature and % crystallinity of the these two composites system increases at low fluence and then decreases on further increase of fluence. It means that polymer composite improved the crystallinity at low fluence and tends to change into the amorphous phase on further increase of the fluence. This result is confirmed by the thermal analysis (DSC) result of these two composites.

AFM study reveals that the average surface roughness increases after irradiation in all cases due to large sputtering effect from the surface of films because of SHI interaction.

The agglomeration of the particles increased on increasing the concentration of fillers and connectivity increased further upon irradiation as revealed from SEM analysis for all composites, which is also confirmed by conductivity results.

Reference

[1]Q. M. Zhang, V. Bharti, and X. Zhao, Science 280 (1998) 2101.

[2]Q. M. Zhang, H. F. Li, M. Poh, X. Feng, Z. Y. Cheng, H. S. Xu, and C. Huang, Nature (London) 419 (2002) 285.

[3]F. Xia, Z. Y. Cheng, H. S. Xu, H. S. Li, and Q. M. Zhang, Adv. Mater. (Weinheim, Ger.) 14 (2002) 1600.

[4]Y. Bai, Z. Y. Cheng, V. Bharti, H. S. Xu, and Q. M. Zhang, Appl. Phys. Lett. 76 (2000) 3804.

[5]H. Banno and K. Ogura, Ferroelectrics 95 (1989) 111.

[6]Z. M. Dang, L. Z. Fan, Y. Shen, and C. W. Nan, Chem. Phys. Lett. 369 (2003) 95.

[7] Z. M. Dang, Y. Shen, and C. W. Nan, Appl. Phys. Lett. 81 (2002) 4814.

[8] Z. M. Dang, J. B. Wu, L. Z. Fan, and C. W. Nan, Chem. Phys. Lett. 376 (2003) 389.

[9] C.-W. Nan, Prog. Mater. Sci. 37 (1993) 1.

[10] A. L. Efros and B. I. Shklovskii, Phys. Status Solidi B 76 (1976) 475.

[11] D. J. Bergman and Y. Imry, Phys. Rev. Lett. 39 (1977) 1222.

[12] C. Pecharroman and J. S. Moya, Adv. Mater. (Weinheim, Ger.) 12 (2000) 294.

[13] C. Pecharroman, E. B. Fatima, and J. S. Moya, Adv. Mater. (Weinheim, Ger.) 13 (2001) 1541.

[14] Z.M.Dang, Ce-Wen, D. Xie, Yi-He. Zhang, S.c.Tjong, Appl. Phys. Lette. 85(2004) 97.

[15] D.Stauffer. 1984, Introdution of percolation theory, London: Taylor & Francis.

[16] F. Lux, J.Mater Sci. 28(1993) 285-301.

[17] A.L. Evelyn, D. Ila, R.L. Zimmerman, K. Bhat, D.B. Poker, D.K. Hensley, Nucl. Instr. And Meth. B 127–128 (1997) 694.

[18] N.L.Singh, Dolly Singh, Anjum Qureshi, Radiation Effect and defects in solids 166(8:9)640 (2011) 647.

[19] Dolly Singh, N. L. Singh, P. Kulriya, A. Tripathi, D. M. Phase , J. Composite Materials 44(2010)3165-3178.

[20] Anjum Qureshi, Dolly Singh, Sejal Shah, N.L.Singh, Mehmet Eroglu, Arif N. Gulluoglu

Proceedings of the DAE Solid State Physics Symposium Volume 52 (2007) 181

[21] Dolly Singh, N.L. Singh, A. Qureshi, P. Kulriya, A. Tripathi, D. K. Avasthi, Arif. N. Gulluoglu, Non. Crystalline and Solids 356 (2010) 856.

[22] Z. M. Elimat , J. Phys. D: Appl. Phys. 39(2006) 2824.

[23] Y. P. Mamunya, V.V. Davydenko, P. Pissis, E. V. Lebedev.Eur Poly J.38(2002)1887. [24] N.L. Singh, Sejal Shah, Anjum Qureshi, P.K.Kulariya,D.K.Avasthi and A.M.Awasthi, Radiation Effects & Defects in Solids 164(2009) 619.

[25] P. Dutta, S. Biswas, M. Ghosh, S. K. De and S. Chatterjee, Synth. Met., 122 (2000) 455-461

[26] I.O.Ayish and A.M. Jihlif, Journal of Reinforced plastics & composites 29(2010) 3237-3243.

[27] Z. Dang, Y. Zhang, S. Tjong, Synth. Met. 146(2004) 79-84.

[28] J. Dyre, T. Schrøder, Rev. Modern Phys. 72 (2000)873-892.

[29] J. Meyer, Polymer Engineering and Science, 13 (1973) 462–468.

[30] M.A.Berger, R.L. McCullough, Compos Sci Technol 1985, 22, 81.

[31] N.P. Bogoroditsky, V.V Pasynkov, B.M. Tareev, Electrical engineering materials, 1974 (Moscow: Mir publisher)

[32] X . Yan, T. Xu, S. Xu, S.Wang, S. Yang, Nanotechnology. 15 (2004)1759.

[33] A. Atta, J Polym. Matter 52(2001) 361.

[34] L. C. Costa, M. Valente, M. A. Sa, F. Henry, Polym. Bullet. 57(2006) 881.

[35] Z. M. Elimat, A.M Zihlif, G. Ragosta, J. Phys. D. Appl. Phys. 41(2008) 165408.

[36] H. P. De Oliveira, M.V.B. dos Santos, C.G. dos Santos, C.P. de Melo. Mater. Charact., 50(2003) 223-226

[37] H. P. de Oliveira, M.V.B. dos Santos, C.G. dos Santos, C.P. de Melo, Synth. Met., 135-136(2003) 447-448

[38] D. S. McLachlan, B. H. Michael, Phy. Rev. B 60 (1999) 12746-12751.

[39] A. Qureshi, A. Mergen, S. E. Mehmet, A. Gulluoglu, N. L. Singh, J Macromol Sci A, 45(2008) 462-469.

[40] M.A. Berger, R.L. McCullough Compos. Sci. Technol. 22(2) (1985) 81-106.

[41] Scherrer P. Gott Nachar 2 (1918) 98.

[42] G. Kemeny, S. D. Mahanti, Proc. Nat. Acad. Sci USA,Vol 72,pp. 999. 1975.

[43]V. Singh, A. R. Kulkarni and T. R. Rama Mohan, J. Appl. Polym. Sci. 90 (2003) 3602–8.

[44] H. Zois, L. Apekis, Y. P. Mamunya J. Appl. Polym. Sci. 88(2003) 3013–20.

[45] X. Y. Huang, P. K. Jiang, C. U. Kim, Journal of Applied physics 102(2007) 124103.

[46] Y. Shen, Z. X. Yue, M. Li and C.W. Nan, Adv. Funct. Mater. 15:7(2000) 1100-1103.

[47] E. H. Lee, G. R. Rao and L. K. Mansur, Materials Science Forum 248-249(1997)135-146.

[48] I. V. Kityak. J. Non-Crystalline Solids, 292 (2001) 184-201.

[49] R. C. Ramola,, Abdullah Alqudami, Subash Chandra, S. Annapoorni, J. M. S. Rana, R. G. Sonkawade, Fouran Singh and D. K. Avasthi, Radiation Effects & Defects in Solids 163(2008) 139–147.

[50] A. Tager, 1978 Physical chemistry of polymers (Moscow: MIR Publishers).